EFFECT OF SELECTED PHYSICAL AND CHEMICAL PARAMETERS ON CRYSTAL VIOLET DECOLORIZATION BY IMMOBILIZED LACCASE

NUR ATIQAH ISMAIL

SGF 070021

IN PARTIAL FULFILMENT OF THE REQUIREMENT FOR THE DEGREE OF MASTER OF BIOTECHNOLOGY

INSTITUTE OF BIOLOGICAL SCIENCES
FACULTY OF SCIENCE
UNIVERSITI MALAYA
KUALA LUMPUR
MALAYSIA

2010

ABSTRACT

Synthetic dyes are used for coloration of various materials like textiles, leather and food. Wastewater from dyeing industries constitutes a threat to the environment as many synthetic dyes are often toxic, mutagenic and carcinogenic. Besides, light absorption is hindered by the dyes run-off creating problems to photosynthetic aquatic plants and algae. Biodegradation of waste dyestuff with enzymes provides a viable alternative compared to the often expensive physical/chemical methods. Laccase from *Trametes versicolor* was chosen in this study as it exhibits low substrate specificity and high ability to oxidize many pollutants which suggested its potential in wastewater treatment and bioremediation. The enzyme was immobilized using calcium-alginate entrapment method. Calcium-alginate entrapment profile was generated to determine the optimum immobilization condition. The observed loading efficiency was greater than 90%. Triphenylmethane dye i.e. Crystal violet was used in this study and decolorization of crystal violet was followed using spectrophotometer. Variables for efficient dye decolorization *viz.* initial dye concentration (ppm), agitation speed (rpm) and process time (day) were optimized using response surface methodology (RSM) Box-Behnken design protocol. The optimization of process parameters were monitored in a working volume of one hundred milliliters (100 ml) in shake flasks to study the maximum decolorization of crystal violet using the enzyme. Under optimal condition (60 rpm, 5 ppm and within 2 days) high percentage of crystal violet decolorization (40%) was observed. Experiments were scaled-up to two liters (2 L) stirred tank reactor (STR) to examine the effect of impeller types (60° angled blade and 180° curved blade) towards percentage of decolorization. At high speed (160 rpm), 60° angled blade (axial impeller) was better compared to 180° curved blade for both high (30 ppm) and low (5 ppm) initial dye concentration. Conversely, at low speed (60 rpm), axial impeller is better than curve for low initial dye concentration (5 ppm). However, at high initial dye concentration (30 ppm) there was no significant effect in percentage of dye decolorization for both impellers. By choosing appropriate impellers in STR operation, the percentage of crystal violet decolorization can be improved.

ABSTRAK

Pewarna sintetik selalu digunakan untuk mewarna pelbagai bahan contohnya dalam industri tekstil, kulit dan makanan. Air buangan daripada industri terbabit boleh menyebabkan pencemaran kepada alam sekitar kerana pewarna sintetik selalunya toksik, mutagenik dan karsinogenik. Selain daripada itu, air buangan pewarna menghalang penyerapan cahaya matahari ke dasar sungai atau laut lalu menyebabkan masalah fotosintesis kepada algae dan tumbuhan-tumbuhan di dasar. Biodegradasi air buangan pewarna oleh enzim merupakan satu alternatif yang praktikal berbanding biodegrasi menggunakan bahan kimia atau fizikal. Enzim lakase telah dipilih untuk digunakan dalam ujikaji ini kerana ia mempunyai substrat spesifikasi yang rendah dan mampu untuk mengoksida pelbagai jenis bahan cemar. Oleh sebab itu, enzim ini mempunyai potensi untuk merawat air buangan dan bioperubatan. Enzim ini telah disekat gerak menggunakan kaedah kalsium-alginat sekat gerak. Profil kalsium-alginat dibuat untuk menentukan keadaan sekat gerak yang optimum. Muatan efisien adalah lebih daripada 90% untuk setiap kali kaedah sekat gerak dilakukan. Pewarna triphenilmethana iaitu violet kristal (Crystal Violet) telah digunakan dalam ujikaji ini dan penyahwarnaan violet kristal diikuti dengan mengunakan spektrophotometer. Pembolehubah yang dikaji untuk penyahwarnaan yang effisien adalah kepekatan asal pewarna (ppm), kelajuan putaran setiap minit (rpm) dan masa (hari). Pembolehubah-pembolehubah ini dioptimumkan menggunakan kaedah tindakbalas permukaan (response surface) Box-Behnken. Proses untuk mengoptimumkan pembolehubah dilakukan dengan menggunakan seratus milliliter (100 ml) pewarna dalam bikar. Dalam keadaan yang optimum (60 rpm, 5 ppm dan selama 2 hari) penyahwarnaan yang optimum telah diperolehi. Seterusnya, isipadu ditingkatkan kepada dua liter (2 L) dalam tangki reaktor pengacauan (STR) untuk mengkaji dua jenis pengacau (60° bilah rata axial dan 180° bilah lengkuk) terhadap peratusan penyahwarnaan. Pada putaran yang laju (160 rpm), bilah axial adalah lebih baik untuk digunakan berbanding dengan bilah lengkuk untuk kepekatan pewarna yang tinggi (30 ppm) dan rendah (5 ppm). Walau bagaimanapun, pada putaran yang perlahan (60 rpm), bilah axial adalah lebih baik daripada bilah lengkuk hanya untuk kepekatan pewarna yang rendah (5 ppm), untuk kepekatan pewarna yang tinggi pula, tiada kesan yang ketara diantara kedua-dua bilah pengacau. Dengan memilih bilah pengacau yang bersesuaian dalam operasi tangki reaktor pengacau (STR), peratusan pewarnaan violet kristal dapat dipertingkatkan.

LIST OF FIGURES

LIST OF TABLES

LIST OF ABBREVIATIONS

Abs	Absorbance
ANOVA	Analysis of variances
$CaCl_2$	Calcium chloride
cm	Centimeter
et al.	et alia (and others)
K_m	Michaelis constant
L	Liter
M	Molar
m	Milli
mg	Miligram
mm	Milimeter
min	Minutes
ppm	Part per million = mg/L
rpm	Revolution per minute
RSM	Response surface methodology
STR	Stirred tank reactor
U	Enzyme unit
v	Initial reaction velocity
V_{max}	Maximum reaction velocity
w/v	Weight per volume
v/v	Volume per volume
$[E]$	Enzyme amount
$[S]$	Substrate concentration
^0C	Degree Celsius
µ	Micro

CHAPTER 1

INTRODUCTION

Dyes are complex aromatic compounds that are normally used for coloration of various substrates like textiles, leather and papers. Wastewater from dye-based industries constitutes a threat to the environment (Couto & Toca, 2006) as many synthetic dyes are often toxic, mutagenic and carcinogenic. Besides, certain chromophores can have negative impact on photosynthetic aquatic plants and algae because of light diffusion reduction (Trovaslet *et al.*, 2007).

Dye-based effluents are normally not amenable to conventional biological wastewater treatment due to recalcitrant, persistent and non-biodegradable nature. Among the chemical classes of dyes, triphenylmethane and azo dyes have widespread industrial used, yet they are not readily biodegradable (Pointing & Vrijmoed, 2000). Besides conventional chemical and physical methods, the possibility of using biological method with white rot fungi for dye decolorization has attracted significant attention in the last decade. Biodegradation studies using liquid fungal cultures and purified ligninolytic enzymes, e.g. laccases, manganese-dependent peroxidases (MnP), and lignin peroxidases (LiP), proved the capacity of white rot fungi to degrade synthetic dyes as well as other types of organic pollutants (Stolz, 2001).

This research was focused on utilizing laccase from *Trametes versicolor* for Crystal violet decolorization. Laccase is a multicopper oxidase that reduces oxygen to

water and simultaneously mediates the oxidation of various aromatic substrates. Their typical molecular mass ranges from 60 to 85 kDa (Tauber *et al.*, 2005). Laccase is capable of catalyzing a four-electron transfer reaction necessary to reduce molecular oxygen, which is used as the terminal electron acceptor, thus forming water without formation of H_2O_2. Laccase has very broad substrate specificity with respect to the electron donor (Couto & Toca, 2006). The low substrate specificity exhibited by laccase and its ability to oxidize many pollutants suggested its potential in wastewater treatment and bioremediation.

Recent studies have shown that many industrial dyes can be decolorized by fungal laccase. One of the main drawbacks of using free enzymes in wastewater treatment is their instability during reaction, due to the wide variety of environmental conditions and complexity of the effluent. The immobilization of enzymes to microcapsules or water-insoluble supports can increase their operational stability and durability at high pH, tolerance to elevated temperatures and to make the enzyme less vulnerable to inhibitors, such as copper (Cu) chelators. Furthermore, enzyme immobilization would allow the reuse of the enzyme and thus decrease the cost of industrial applications (Srikanlayanukul *et al.*, 2006). Therefore, many efforts have been made to immobilize laccase.

Among the various immobilization techniques such as adsorption, entrapment and crosslinking, the entrapment method may be a good choice for enzyme immobilization, as the process of entrapment is mild and causes relatively little damage to the enzyme native structure. Alginate is one of the most frequently used polymers for immobilization

and microcapsulation technologies (Sriamornsak & Sungthongjeen, 2007). Alginate is an anionic polymer composed of α-L-guluronic acid and β-D-mannuronic acid. Enzyme can be entrapped in alginate beads produced by the crosslinking between α -L-guluronic acid and divalent cations such as calcium (Lu *et al.*, 2007).

In this study, selected parameters hypothesized to influence Crystal violet decolorization were studied. The three (3) parameters selected for investigation are the initial Crystal violet concentration, the reaction time and the agitation rate. Statistical design (response surface methodology, Box-Benhken design) using different combinations of the three parameters was employed in this study to optimize the process parameters. A total of forty-five (45) replicated combinations were tested. Data obtained were subjected to statistical analyses and then fitted to a regression model for optimization. The kinetic of the Crystal violet decolorization was described using Michaelis-menten model. In a scale-up studies using stirred tank reactor, a range of impeller speeds and geometries was employed to analyze the mixing effect on Crystal violet decolorization by immobilized laccase.

The objectives of this study were:

1. to study the Crystal violet decolorization using immobilized laccase under selected physical parameters;
2. to determine the optimum conditions for enzyme activity *via* statistical design of experiment (response surface methodology);
3. to develop kinetic model for dye decolorization by immobilized laccase;

4. to study the power consumption of 60° angled blade and 180° curved blade impellers;
5. to study types of impellers (60° angled blade and 180° curved blade) that give greater effect in Crystal violet decolorization.

CHAPTER 2

LITERATURE REVIEW

2.1 Laccase

Laccase (EC 1.10.3.2; benzenediol: oxygen oxidoreductase) was first discovered more than one century ago in the exudates of Japanese lacquer tree, *Rhus venicifera* where it is implicated in wound-response and the synthesis of lignin, the complex polymer that constitutes a main component of the plant cell wall (Antorini *et al.,* 2002). Laccases are widely distributed in nature originating from plants, insects, bacteria and especially fungi (Mechichi *et al.,* 2006). The white rot fungi, which can depolymerize lignin, are the main laccase producers (Zille *et al.,* 2003). The genus *Trametes* is one of the most efficient lignin degraders and in particular, *Trametes versicolor* is the most extensive utilized among them (Couto, 2007).

The idea of using oxidoreductive enzymes for wastewater treatment was developed in early 1980s (Abadulla *et al.,* 2000). Conventional methods of physical or chemical process for the effective removal of phenols, aromatic amines and dyes belonging to different categories are outdated due to certain inherent limitations. Degradation products from chemical or physical approach are sometimes more toxic and hence the laccase enzymatic treatment of dye-containing effluents is preferred over physico-chemical methods (Niladevi & Prema 2008). Besides, the advantage of enzymatic approach is that the rate of decolorization and their removal is quite fast and are less sensitive to operational upsets as compared to the microbial flora (Tauber *et al.*,

2005; Abadulla *et al.*, 2000). Other than that, enzymes can react with a broad range of aromatic compounds under dilute conditions (Abadulla *et al.*, 2000). The catalytic action of enzymes is extremely efficient and selective compared to chemical catalysts due to higher reaction rates, milder reaction conditions and greater stereospecificity. They can catalyze reactions at relatively low temperature and in the entire aqueous-phase pH range. In addition, the application of living white rot fungi which is non reusable and needs sterile condition is very strenuous in industry (Tauber *et al.*, 2005). Though biocatalysts are widely used in several fields, their role in solving the environmental problems has been felt very recently only (Couto, 2007).

Tauber *et al.* (2005) stated that the major reason that enzymatic treatments have not yet been applied on an industrial scale is due to the huge volume of polluted wastewater demanding remediation. Free enzymes suffer from certain drawbacks such as thermal instability, reusability, activity inhibition, susceptibility to attack by proteases, etc. To overcome all these limitations use of immobilized enzyme has been suggested due to its stability and reusability.

2.1.1 Properties of laccase

Laccases belong to the family of blue multicopper oxidases that reduce oxygen to water and concomitantly perform one electron oxidation of many phenolic substrates (Couto, 2007; Zille *et al.*, 2003; Antorini *et al.*, 2002). Laccases catalyze the removal of a hydrogen atom and an electron from the hydroxyl group of polyamines, *ortho*- and *para*-subtituted mono- and polyphenolic substrate to form free radicals (D' Sauza *et al.*, 2006;

Mechichi *et al.*, 2006; Abadulla *et al.*, 2000). Further electron withdrawal will lead to depolymerization, repolymerization, demethylation, or quinone formation (Tauber *et al.*, 2005).

Tauber *et al.* (2005) and Abadulla *et al.* (2000) reviewed that laccases and other blue copper oxidases not only oxidize the phenolic and methoxyphenolic acids, but also decarboxylate them and modify their methoxyl groups by demethylation or demethoxylation. These reactions constitute an important step in the initial transformation of lignin polymer.

The laccases, lignin peroxidase (LiP) and manganese-dependent peroxidases (MnP) are classified as the three major extracellular lignin degrading enzymes produced by the ligninolytic system of some white-rot fungi (D' Sauza *et al.*, 2006; Zille *et al.*, 2003). While LiP cleaves the nonphenolic aromatic bonds of lignin, MnP and the fungal laccases can oxidise the phenolic components of lignin (Antorini *et al.*, 2002).

According to Niladevi & Prema (2008), Vanhulle *et al.*, (2007), Antorini *et al.*, (2002) and Pointing & Vrijmoed (2000) the enzymatic approach to decolorize dye mainly focused on laccases of white rot fungi because:

(i) laccases present a better thermostability than LiP and MnP;

(ii) laccases are oxygen oxidoreductase that can be oxidised by oxygen from air, unlike the LiP and MnP, which require expensive hydrogen peroxide as a co-substrate for activation;

(iii) laccases act less specifically on aromatic rings, thus having potential to degrade a wide range of compounds;

(iv) laccases are often produced in larger amount and often produced constitutively or require less fastidious induction conditions than either LiP or MnP.

Laccase can also catalyze the oxidation of non-phenolic compounds in the presence of synthetic redox mediators such as 3,5-dimethoxy-4-hydroxybenzaldehydazine (Syringaldazine), 2,2'-azino-bis-[3-ethylbenz-thiazoline-6-sulfonic acid] (ABTS), 1-hydroxybenzotriazole (HBT) and phenothiazines (Couto, 2007; Nogala *et al.,* 2007; Abadulla *et al.,* 2000). Although mediators can enhance dye degradation and lignin degradation by laccase, they do not have industrial potential for dye degradation process, since their application is expensive, increases wastewater toxicity and the behaviour of the system can vary significantly with different enzymes or substrates (Kunamnanei *et al.,* 2008; Cameselle *et al.,* 2003). While laccases can eventually be reused by immobilization, mediators are lost with the effluents. As an alternative to artificial redox mediators, natural mediators such as phenol, aniline, 4-hydroxybenzoic acid and 4-hydroxybenzyl alcohol would be preferable as it has been found that natural mediators have been as efficient as ABTS and HBT (Kunamnanei *et al.,* 2008).

Figure 2.1 showed the varying stages of laccase during its reaction with compatible compounds (Wesenberg *et al.*, 2003).

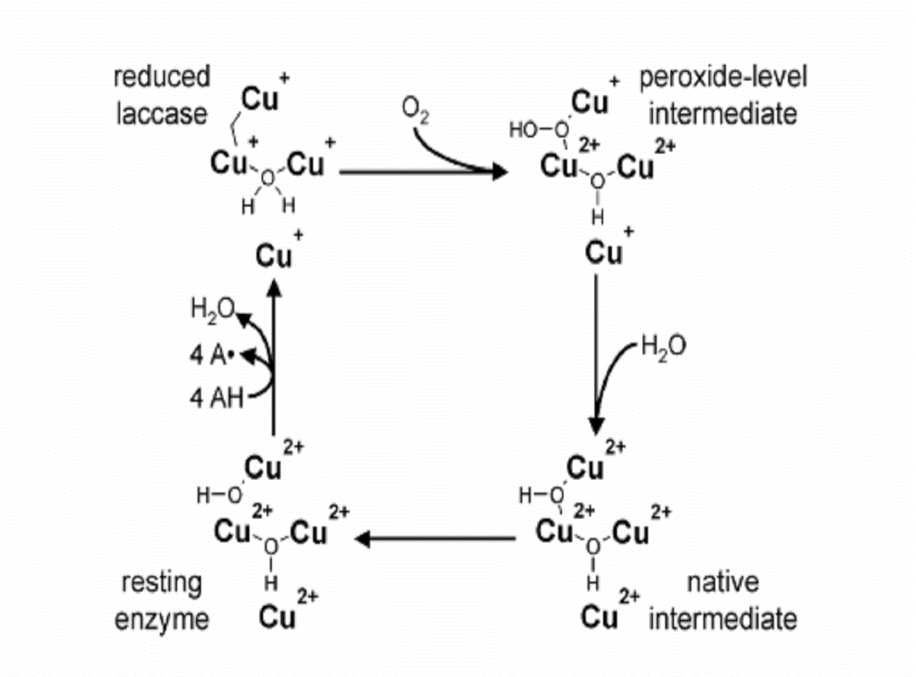

Figure 2.1: Catalytic cycle of laccase with substrates.

2.1.2 Applications of laccase

Due to lack of substrate specificity, laccases proved to be very effective in eliminating aromatic alcohols in industrial colored wastewaters, detoxification of contaminated soil and water, degradation of polycyclic aromatic hydrocarbons (PAHs), delignification of wood-pulp and prevention of wine decoloration (D' Sauza *et al.*, 2006; Tauber *et al.*, 2005; Kandelbauer *et al.*, 2004; Zille *et al.*, 2003). Laccase renders phenolic compounds less toxic *via* degradation or polymerization reactions or cross–coupling of pollutant phenols with naturally occurring phenols (Tauber *et al.*, 2005).

2.1.2.1 Dye decolorization

Synthetic dyes from textile, paper, cosmetics, pharmaceutical, food and several other industries are being discharged to the surrounding environment without any further treatment. Kunamnanei *et al.* (2008) reported that it is estimated that around 10–15% of the total dyes are lost in the effluent during dyeing process and causing extensive pollution. Decolorization of industrial dyes is currently performed by chemical or physical methods including adsorption, coagulation–flocculation, precipitation, ion-exchange, oxidation, electrochemical, chemical degradation or photodegradation. However, these methods are highly expensive, time consuming and mostly not effective which limits their application (Mechichi *et al.,* 2006; Tauber *et al.,* 2005). Dye decolorization is also achieved by routine anaerobic treatment of the effluents in municipal sewage systems (Kunamnanei *et al.,* 2008; D' Sauza *et al.,* 2006).

However, brightly colored, water-soluble reactive and acid dyes are the most problematic, as they tend to pass through conventional treatment systems unaffected. Several of these dyes are resistant to microbial attack due to their complex structure and thus recalcitrant (D' Sauza *et al.,* 2006). Therefore, the enzymatic treatment of industrial effluents containing aromatic compounds becomes necessary prior to their final discharge to the environment.

Studies performed by Mechichi *et al.* (2006), Zille *et al.* (2003) and Yesilada & Ozcan (1998) proved that laccase can degrade several dye structure to transform toxic compounds into safer metabolites and may be useful to control environmental pollution.

The degradation of triphenylmethane dyes have been extensively studied using a wide range of fungi and bacteria but work carried out using enzymes is more limited (Couto, 2007).

Until now, laccases from many different fungi such as *Pycnoporus* strains (Vanhulle *et al.,* 2007), *Pycnoporus sanguineus* (Trovaslet *et al.*, 2007; Pointing & Vrijmoed, 2000), *Pycnoporus cinnabarinus* (Schliephakea *et al.,* 2000), *Trametes hirsuta* (Couto, 2007; Abadulla *et al.,* 2000), *Trametes trogii* (Mechichi *et al.,* 2006), *Trametes villosa* (Zille *et al.,* 2003), *Coriolus versicolor* (Yesilada & Ozcan, 1998) and *Coriolus versicolor* RC3 (Srikanlayanukul *et al.,* 2006) have been described to decolorize a wide structural variety of dyes. Table 2.1 listed the type of dyes that have been decolorized by the laccases originated from various fungi.

Table 2.1: Ability of laccases from different fungi to decolorize wide structural variety of dyes.

Type of dyes	Source of Laccase	References
Anthraquinonic acid dye	*Pycnoporus* strains	Vanhulle *et al.* (2007)
Azo and triphenylmethane dyes	*Pycnoporus sanguineus*	Trovaslet *et al.* (2007) Pointing & Vrijmoed (2000)
Chicago Sky Blue	*Pycnoporus cinnabarinus*	Schliephakea *et al.* (2000)

Derma Carbon NBS, Derma Burdeaux V, Derma Pardo 5 GL and Derma Blue DBN, Sella Solid Blue 4GL and Sella Solid Yellow4GL	*Trametes hirsuta*	Couto (2007)
Triarylmethane, indigoid, azo, anthraquinonic dyes, reactive Blue 221, reactive Black 5, Direct Blue 71, Basic Red 9 Base, Reactive Blue 19, Acid Blue 225, Acid Blue 74	*Trametes hirsute*	Abadulla *et al.* (2000)
Remazol Brilliant Blue R	*Trametes trogii*	Mechichi *et al.* (2006)
Reactive Black 5	*Trametes villosa*	Zille *et al.* (2003)
Orange II	*Coriolus versicolor*	Yesilada & Ozcan (1998)
Wastewater from Batik Industry	*Coriolus versicolor* RC3	Srikanlayanukul *et al.* (2006)

Dye structure has an important effect on the decolourization ability of white rot fungi. With triphenylmethanes, relatively low chemical differences lead to significant variations on the rate of decolourization. Some structural features influencing the biodegradability of azo dyes have also been identified (Trovaslet *et al.*, 2007; Pointing & Vrijmoed, 2000).

Laccases has demonstrated their ability to decolourize several types of dyes including azo, triphenylmethane and anthraquinonic dyes. However, these enzymes may be sensitive to denaturing conditions typically found in dye containing effluents (high salt concentrations, temperature, pH). As a consequence, development of an efficient textile wastewater treatment process using laccases requires the study of its activity and stability of these enzymes under those conditions. Laccases kinetic parameters are usually described against a wide range of substrates. However little is known concerning the kinetic behaviour of laccases against substrates of industrial interest.

2.2 Enzyme Immobilization

Generally, enzymes are biological catalysts that promote the rate of reactions but they are not consumed in reactions, they may be used repeatedly as long as they remain active. Most enzymes cannot withstand changes in temperature, pH, ionic strength and other vigorous conditions. However, enzyme immobilization has emerged as a promising solution to enhance the stability of the enzymes and improve the separation from complex reaction systems so they can be retained and used to catalyze further subsequent feed. The use of an immobilized enzyme makes it economically feasible to operate an

enzymatic process in a continuous mode. The basic idea behind enzyme immobilization is either by covalently bind or entrap the enzyme in a support material, which prevents the enzyme from leaving but allowing the substrates, co-factors and products to permeate.

Numerous methods exist for enzyme immobilization. The overwhelming majority of the methods can be classified into four main categories: matrix entrapment, microencapsulation, adsorption, and covalent binding. Of these methods, matrix entrapment is the focus in this study.

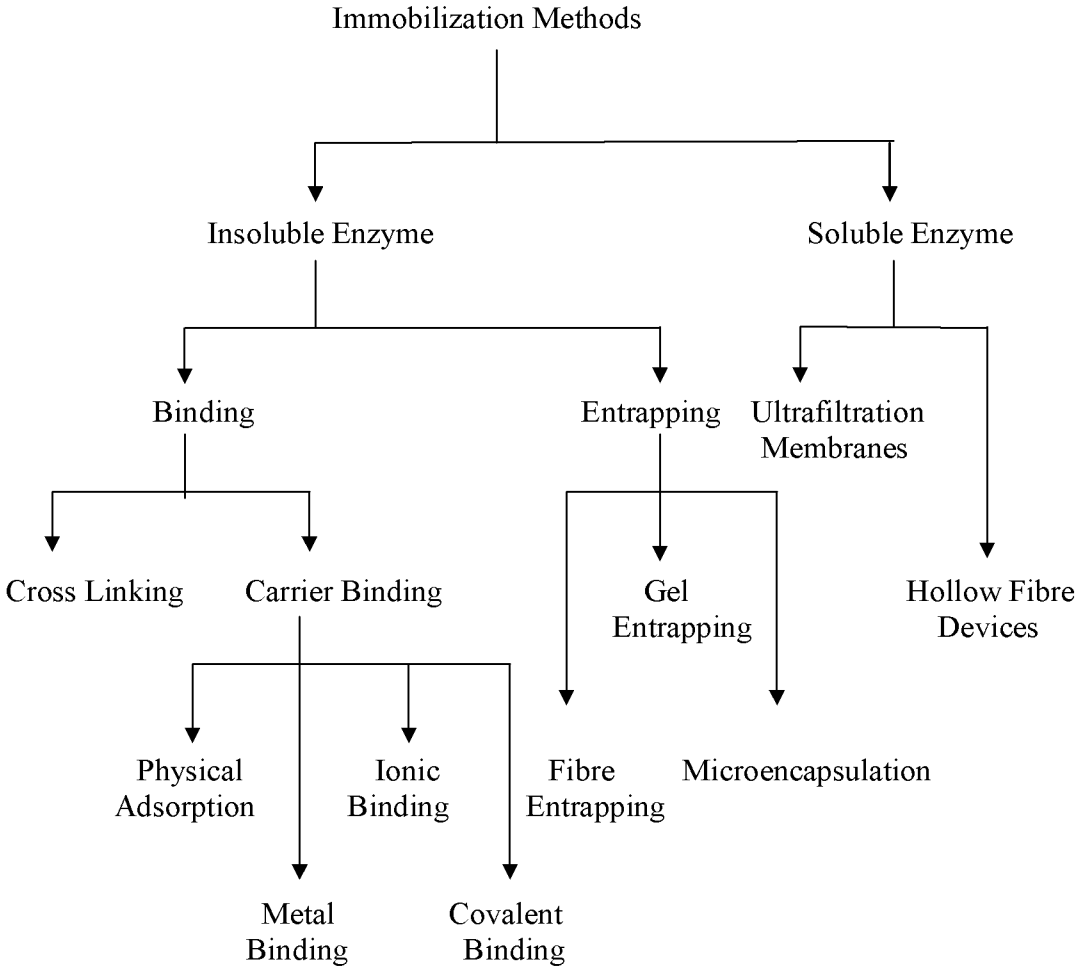

Figure 2.2: Classification of immobilization methods for enzyme (Ivan & Robert, 1994).

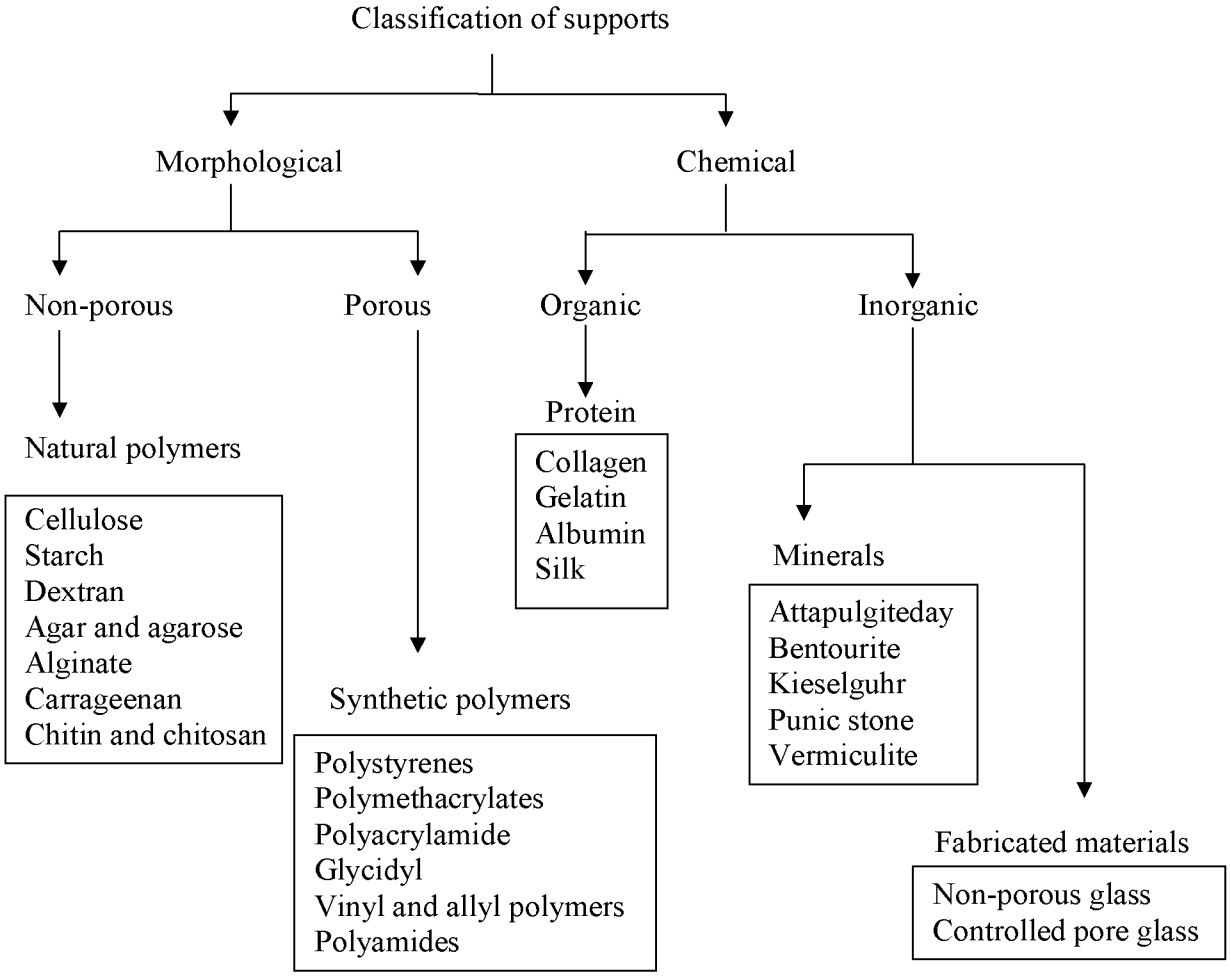

Figure 2.3: Classification of supports for enzyme immobilization according to their morphology or chemical composition (Ivan & Robert, 1994).

Calcium alginate entrapment method is commonly used for enzyme immobilization since the hydrogel is formed under mild conditions. Alginate acid is derived from brown seaweeds (Phaeophyceae). Alginate is a linear copolymer composed of two monomeric units, α-L-guluronic acid and β-D-mannuronic acid (Figure 2.4(a)). According to Sriamornsak & Sungthongjeen (2007), when cross-link agents (calcium ions) are added to a sodium alginate solution, alignment of the G blocks occurs and the calcium ions are bound between the two chains (Figure 2.4 (b)). Depending on the amount of calcium present in the system, these interchain associations can be either temporary or permanent.

a)

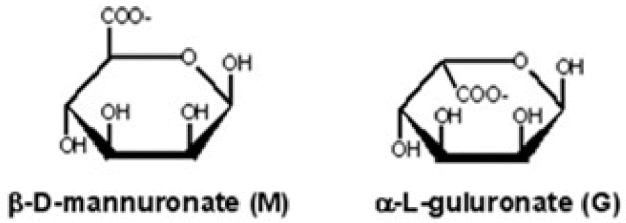

b)

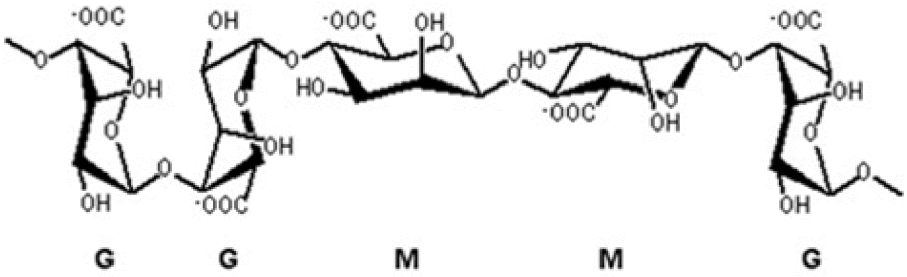

Figure 2.4: Structural design of alginate. (a) Types of monomers in alginate; (b) The structural alginate chain.

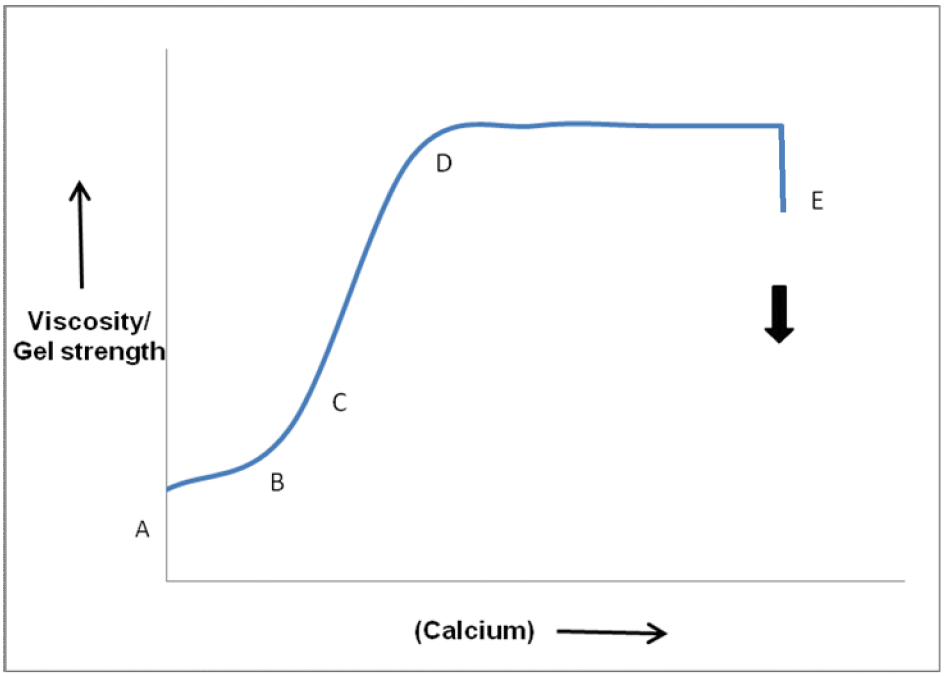

Figure 2.5: The effect of calcium ions on alginate solution.

Based on Figure 2.5, alginate solution may have a certain viscosity (Point A). As calcium ions are gradually introduced into the system they cause the alginate polymer chains to start to align, this is seen as an increase in the solution viscosity (Point B). As more calcium is added the solution viscosity increases to Point C where there is evidence of some gel structure. At this stage, the solution shows thixotropic properties, where it becomes liquid when sheared, pumped or shaken but the structure is regained when shear is removed. As the calcium content in solution increased, thickening, gelation (Point D) and finally precipitation (Point E) occurs as the results from permanent associations of the chains (Sriamornsak & Sungthongjeen, 2007).

Sriamornsak & Sungthongjeen (2007) also stated that the efficiency of an immobilization process can be measured by the following criteria:

(i) high percentage of the enzymes must be initially retained in gel matrices;

(ii) the enzyme activity must be preserved;

(iii)the enzymes must be physically restrained from diffusing back into the substrate solution. This can be achieved by increasing the amount of cross-link agents. However, care should be taken as highly cross-linked matrices can result in higher mass transfer resistances for both the substrate and the product.

2.2.1 Advantages of Immobilization

According to Zille *et al.* (2003), Abadulla *et al.* (2000) and Mosbach (1987), the advantages of immobilized enzymes are as shown in Table 2.2:

Table 2.2: Advantages of immobilized enzyme.

No.	Advantages of Immobilized Enzyme
1.	Recovery and reuse of the enzyme
2.	Increased stability with respect to temperature, time and self degradation
3.	Product obtained is enzyme free
4.	New medical and industrial uses
5.	Use of multi enzyme system
6.	Greater control of catalytic process, permits continuous operation
7.	Modification of properties such as pH optimum and attraction of

	substrate
8.	Reduce the cost
9.	Greater resistance to protease
10.	Less activity inhibition

2.2.2 Limitation of Immobilization

Table 2.3 showed the disadvantages of immobilized enzyme as reported by Zille *et al.* (2003), Abadulla *et al.* (2000) and Mosbach (1987).

Table 2.3: Disadvantages of immobilized enzyme.

No.	Limitation of Immobilized Enzyme
1.	Loss of activity during immobilization due to blockage of active site
2.	Mass transfer problems which is due to steric reactions on substrate accessibility
3.	Enzyme inactivation
4.	Empirical nature of immobilization technology makes it extremely difficult to estimate quantitatively
5.	Possible requirement of higher quality feedstock

2.3 Crystal violet

There are many structural varieties of dyes depending on the type of chromophore (part of the molecule responsible for its color), such as azo, anthraquinone, heterocyclic, triphenylmethane, acridine, arylmethane, cyanine, phthalocyanine, nitro, nitroso, quinone-imine, thiazole or xanthene dyes (Kunamnanei *et al.*, 2008; Mechichi *et al.*, 2006). On the basis of dyeing process, textile dyes are classified as reactive dyes, direct dyes, disperse dyes, acid dyes, basic dyes and vat dyes (Kunamnanei *et al.*, 2008).

2.3.1 Structure of Crystal violet

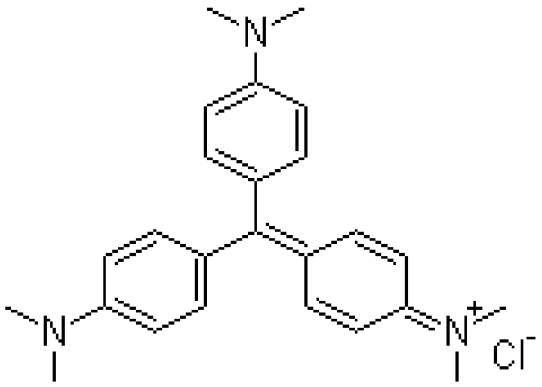

Figure 2.6: Molecular structure of Crystal violet.

Crystal violet is a triphenylmethane dye that is also known under the name of gentian violet. Triphenylmethane dye represent an especially recalcitrant class of compounds. The Crystal violet color is due to the extensive system of alternating single and double bonds (Figure 2.6) which extends over all three benzene rings and the central carbon atom. This alternation of double and single bonding is termed conjugation, and molecules that have extensive conjugation are usually highly colored. In the reaction

product, the three rings are no longer in conjugation with one another, and hence the material is colorless (Kandelbauer *et al.*, 2004).

2.4 Enzyme kinetics

The kinetics of most enzyme reactions can be represented by Michaelis-Menten equation. Michaelis-Menten scheme defines the relationship between the rate of enzyme catalyzed reaction and the concentration of the substrate which can be written as:

$$v = \frac{V_{max} \bullet [S]}{K_m + [S]} \qquad \text{Equation (1)}$$

where v = volumetric rate of reaction

V_{max} = maximum rate of reaction at infinite reactant concentration

K_m = Michaelis constant for the reactant

$[S]$ = concentration of substrate

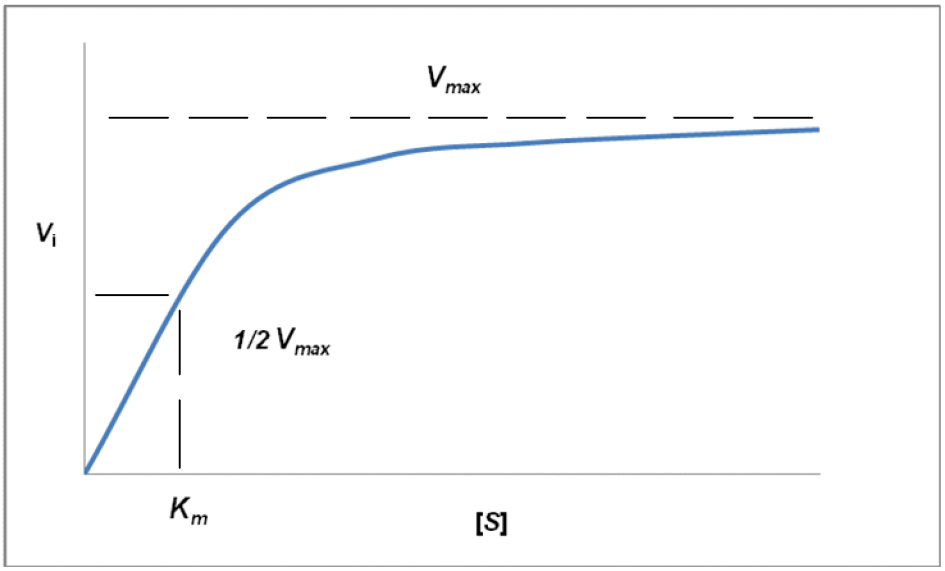

Figure 2.7: Michaelis-Menten plot.

The Michaelis constant K_m is equal to the reactant concentration at which $v = V_{max}/2$, assuming that the reaction rate is not inhibited by the presence of the product. Generally, the rate of enzyme catalyzed reaction is influenced by temperature, pH of the reaction mixture, concentration of substrate and enzyme. Under conditions where the temperature, the pH, the concentration of enzyme and other variables are held constant, the rate of reaction increases on increasing [*S*] but becomes constant at saturating [*S*]. The Michaelis-Menten plot (Figure 2.7) demonstrates that as the substrate increases, the velocity increases hyperbolically, and approaches a maximum rate known as V_{max} (Claeyssens *et al.*, 1989; Sattler *et al.*, 1989). This is dependent upon saturation of the enzyme.

At V_{max}, all enzyme molecules are complexed with substrate, and thus any additional substrate added to the reaction has no effect on the rate of reaction. However, if the enzyme concentration is altered, V_{max} will also change. Thus, V_{max} is not a constant value, but is constant only for a given enzyme concentration. If multiple plots of enzyme activity *versus* substrate concentration are made with increasing enzyme concentration, the value of V_{max} continues to increase, but the K_m remains constant (Norton *et al.*, 1994).

2.4.1 Determination of enzyme kinetic parameters, K_m and V_{max}, using linearization and non-linear regression methods

There are four types of linearization methods; Lineweaver-Burk, Eddie-Hofstee, direct linear and Langmuir plots. The linearization process used in Lineweaver-Burk plot distorts the experimental error in v resulted in the errors are being amplified at low

substrate concentrations. Hence, Lineweaver-Burk plot often gives inaccurate results and therefore not recommended. The second linearization method, Eadie-Hofstee plot can be subject to large errors since both coordinates contain v, but there is less bias at low [S] and consequently, this method has reduced accuracy. The direct linear plot is claimed to be as the easiest model to construct among the others as it composed of entirely of straight lines and requires no calculation or mathematical table (Segel, 1975). The kinetics parameters such as K_m and V_{max} can be determined directly from the plot without any calculation. However, Doran (1995) explained that the direct linear plot was relatively insensitive due to individual erroneous upon reading, which may be far from the correct value. The fourth method, Langmuir plot minimizes distortions in experimental error and therefore this plot is recommended for evaluation of V_{max} and K_m.

Table 2.4: Linerization methods for obtaining kinetic parameters, V_{max} and K_m.

Linerization methods	Equation	Slope and intercept	
Lineweaver-Burk	$\frac{1}{v} = \frac{K_m}{V_{max}[S]} + \frac{1}{V_{max}}$	Slope	$\frac{K_m}{V_{max}}$
		Intercept	$\frac{1}{V_{max}}$
Eadie-Hofstee	$\frac{v}{[S]} = \frac{V_{max}}{K_m} - \frac{v}{K_m}$	Slope	$\frac{1}{K_m}$
		Intercept	$\frac{V_{max}}{K_m}$
Langmuir	$\frac{[S]}{v} = \frac{K_m}{V_{max}} + \frac{s}{V_{max}}$	Slope	$\frac{1}{V_{max}}$
		Intercept	$\frac{K_m}{V_{max}}$
Direct linear	$\frac{V_{max}}{v} - \frac{K_m}{[S]} = 1$		-

There are lot of problems encountered if linearization methods are used to obtained kinetic parameters V_{max} and K_m. The non-linear regression method provides an alternative for getting more accurate values of V_{max} and K_m and minimizing the errors. The non-linear regression is usually used to fit the best curve rather than fit the best line to the data if compared with linear regression. However, the drawback of non-linear model is that the calculations are sometimes sophisticated and require a computer. The lack of knowledge in analyzing and interpreting the data presented by the software may limit the evaluation of the results obtained. Examples of non-linear regression softwares are Polymath® 6.0 and Lucenz (III) (Shacham & Brauner, 2008).

2.5 Response surface methodology (RSM)

Response surface methodology (RSM) is a combination of statistical and mathematical methods that are useful for the modeling and analyzing process parameters. RSM is usually chosen when curvature is suspected in the response surface. This method developed in early 1950s with the main objective is to determine optimum operating conditions in a multivariable system. The optimum could be either a maximum or a minimum of a function of the design parameters. RSM also quantifies the relationship between the parameters and the response surfaces (Montgomery, 2001).

RSM may be employed to:

(i) find the operating conditions that produce the best (optimum) response;

(ii) find factor settings that satisfy operating or process specifications;

(iii)identify new operating conditions that produce demonstrated improvement in product quality over the quality achieved by current conditions;

(iv)model a relationship between the quantitative factors and the response.

The advantages of using experimental design methodology are; it is an economical way for extracting the maximum amount of complex information, a significant experimental time saving factor, it saves the material used for analyses and reduced the personal costs as well (Aslan & Cebeci, 2007). Furthermore, the analysis performed on the results is easily realized and experimental errors are minimized. Statistical methods measures the effects of change in operating variables and their mutual interactions on the process through experimental design method.

The optimization procedures of RSM involves four steps:

(i) designing the experiments for adequate and reliable measurement of the response of interest;

(ii) developing the second order response surface model with the best fittings;

(iii)finding the optimal combination of variables that produce a maximum or minimum value of response;

(iv)representing the direct and interactive effects of variables through two or three dimensional plots.

If all variables are assumed to be measurable, the response surface can be expressed as stated below:

$y = f(x_i, x_{ii}, x_{iii}, \ldots\ldots, x_k) + \square$ Equation (2)

where y = the response;

$x_i, x_{ii}, \ldots, x_k$ = the variables of action called factors;

$\square$ = experimental error.

The goal is to optimize the response y. It is assumed that the independent variables are continuous and controllable by experiments with negligible errors. If a suitable approximation for the true functional relationship between independent variables and the response surface needed to be find, normally a second-order model is utilized in response surface methodology (Montgomery, 2001; Segel, 1975).

$$y = \beta_0 + \sum_{i=1}^{k} \beta_i x_i + \sum_{i=1}^{k} \beta_{ii} x_i^2 + \sum_{i=1}^{k-1} \sum_{j=2}^{k} \beta_{ij} x_i x_j + \epsilon$$ Equation (3)

where y = the response;

x_i, x_j = the input factors (variables) which influence the response y;

$\beta_0, \beta_i, \beta_{ii}$ and β_{ij} = constant regression coefficients of the model;

ϵ = the experimental error.

The β coefficients, which should be determined in the second-order model, are obtained by the least square method that minimize the sum of squares of the model errors. Then, the response surface analysis is done in terms of the fitted surface. If the fitted surface is an adequate approximation of the true response function y, then analysis of the fitted surface will be in the vicinity of equivalent to analysis of the actual system. Consequently, RSM will lead the experimenter rapidly and efficiently to the general vicinity of the optimum (Montgomery, 2001).

2.5.1 Box-Benhken

Box-Behnken designs are experimental design of RSM. The illustration below shows a three-factor Box-Behnken design for fitting response surfaces. Points on the diagram represent the experimental runs that should be performed:

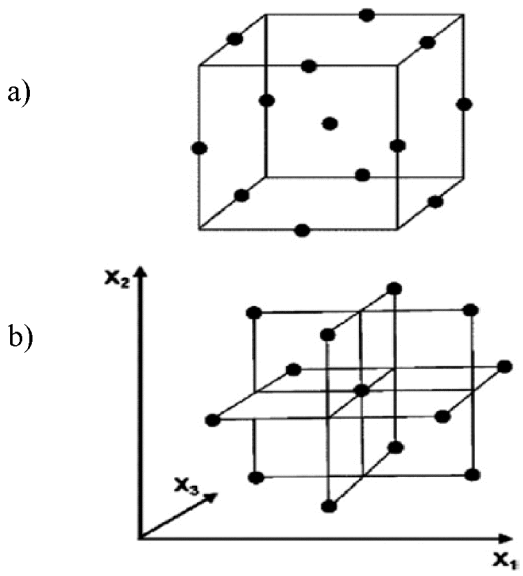

Figure 2.8: Box–Behnken experimental design for 3 factors. (a) The design is derived from a cube; (b) illustration as interlocking 2^2 factorial experiments.

Box–Behnken is a spherical, rotatable second-order designs based on three-level incomplete factorial designs. Viewed as a cube (Figure 2.8(a)), it consists of a central point and the middle points of the edges. However, it can also be viewed as consisting of three interlocking 2^2 factorial design and a central point (Figure 2.8(b)). Box-Behnken designs allow efficient estimation of the first and second-order coefficients (Montgomery, 2001). Because these designs have fewer point combinations, they are less expensive to run than central composite designs (CCD) with the same number of factors.

Box-Behnken designs are really useful if the range of operating zone for the process are known. CCD usually have axial points outside the cube (unless we specify a factor that is less than or equal to one). These points may not be in the region of interest, or may be impossible to run because they are beyond safe operating limits. Box-Behnken designs do not have axial points, hence, it can be sure that all design points fall within the safe operating zone. Box-Behnken designs also ensure that all factors are never set at their high levels simultaneously (Aslan & Cebeci, 2007). It has been applied for optimization of several chemical and physical processes. For examples, modeling of grinding for some Turkish coals (Aslan & Cebeci, 2007), optimization of dye decolorization by commercial laccase (Tavares *et al.*, 2009) and laccase mediated degradation of 2,4- dichlorophenol (Bhattacharya & Banerjee, 2008).

CHAPTER 3

MATERIALS AND METHODS

3.1 Materials

Laccase from Fluka (Germany) with a nominal specific activity of 0.8 U mg^{-1} was used without further purification for the experiments. Sodium alginate (smaller than 200 mesh) was purchased from Fluka (Norway). The viscosity was over 0.02 Pa.s when dissolved to form a 1% (w/v) aqueous solution at 25 ± 1°C. Natrium dihydrogen phosphate-2-hydrate-reinst ($NaH_2PO_4.2H_2O$) from Merck and disodium hydrogen phosphate (Na_2HPO_4) from R & M Chemicals were used to make phosphate buffer at pH 5. Calcium chloride ($CaCl_2$) from Systerm (ChemPur) was used as crosslinking agent for alginate. Syringaldazine (Sigma, Germany) was used to assay the enzyme activity. Crystal violet dye was purchased from BDH Chemicals (United Kingdom). Other reagents used were of analytical grade.

Equipments:

1) UV/VIS Spectrophotometer Jasco V-630 (Japan) and quartz cuvettes with 1 cm light path;
2) IKA® Werke Eurostar Digital Mixer, 50-2000 rpm (Germany);
3) Daihan LabTech Shaker (Korea);
4) Dino-Lite Digital Microscope (Taiwan).

3.2 Determination of free laccase activity assay using syringaldazine

Syringaldazine was used as a substrate for spectrophotometric determination of laccase activity. Laccase activity was determined at 25 ± 1°C by monitoring the rate of oxidation of syringaldazine to the colored tetramethoxy-azobis methylenequinone (Schliephake *et al.*, 2000). One activity unit was defined as the amount of laccase that oxidized 1 µmol of syringaldazine per min. Reagents needed were 50 mM phosphate buffer (pH 5), 0.1 mM syringaldazine solution (in 50% ethanol) and appropriate dilution of laccase. The assay mixture contained 0.2 ml of 0.1 mM syringaldazine, 3 ml of phosphate buffer pH5, and 0.2 ml of an appropriate laccase solution (0.005, 0.008, 0.01, 0.03 and 0.05 U). The blank was prepared using 3.2 ml phosphate buffer pH 5 and 0.2 ml syringaldazine (Table 3.1). Total reaction volume for both sample and blank were 3.4 ml.

Table 3.1: Typical components of reaction mixture for laccase assay.

Solution	Test	Blank
50 mM Phosphate buffer pH 5	3.0 ml	3.2 ml
0.1 mM Syringaldazine (in 50% ethanol)	0.2 ml	0.2 ml
Enzyme solution	0.2 ml	-
Total volume	3.4 ml	3.4 ml

Three replicates were made for each enzyme activity measurement. The solutions were then assayed using UV/VIS Spectrophotometer Jasco V-630 (Japan) at a wavelength of 530 nm for 10 minutes at 25 ± 1°C.

Determination of reaction rate of laccase

Enzyme activity was calculated as follows:

The initial reaction rate was obtained as a change of absorbance per minute ($\Delta Abs\Delta min^{-1}$). This value was then converted to the concentration of the substrate (syringaldazine) by using Lambert-Beer law (Schmid, 2001):

$$A = k*c*L \qquad \text{Equation (4)}$$

where A = absorbance

k = extinction coefficient of laccase (65000 $M^{-1}cm^{-1}$)

c = concentration of the substrate

L = light path length (1cm).

t = time (minutes)

$$\frac{dA}{dt} = k* L*\frac{dc}{dt} \qquad \text{Equation (5)}$$

where dA/dt = the rate of change in absorbance

dc/dt = the rate of change for the substrate

$$\frac{dc}{dt} = \frac{dA}{dt} * \frac{1}{k*L} \qquad \text{Equation (6)}$$

Hence, $\frac{dc}{dt} = \frac{dA}{dt} * \frac{1}{65000\ M^{-1}\ cm^{-1} * 1\ cm} = M\ min^{-1}$

$M\ min^{-1} = mol\ L^{-1} min^{-1}$

Enzyme unit is defined as micro mole per minute (µmol min^{-1}). To convert M min^{-1} into µmol L^{-1} min^{-1} the following relationship was used:

$M\ min^{-1} = 10^6\ \mu mol\ L^{-1}\ min^{-1}$ Equation (7)

The concentration obtained in M min^{-1} was converted to µM min^{-1} and this value was plotted against different enzyme concentrations. Similar calculation was used to obtain initial rate of reaction at different syringaldazine concentrations.

Determination of percentage of product formation

The percentage of product formation (%) within 10 seconds was calculated using Equation (8). The initial syringaldazine (substrate) concentration used in this experiment was 0.1 mM.

$$\text{Percentage of product formation (\%)} = \frac{\text{Initial rate of reaction}}{\text{min}} * \frac{1\ \text{min}}{60\ \text{sec}} * 10\ \text{sec}$$

Equation (8)

3.3 Determination of Crystal violet spectrum and standard curve preparation

The Crystal violet spectrum was obtained using spectrophotometer and analyze in visible light wavelength ranging from 400 to 900 nm. The Crystal violet dye absorbs most strongly at 590 nm as indicated by the sharp peak (Figure 3.1). This wavelength value was used for the entire dye decolorization assay.

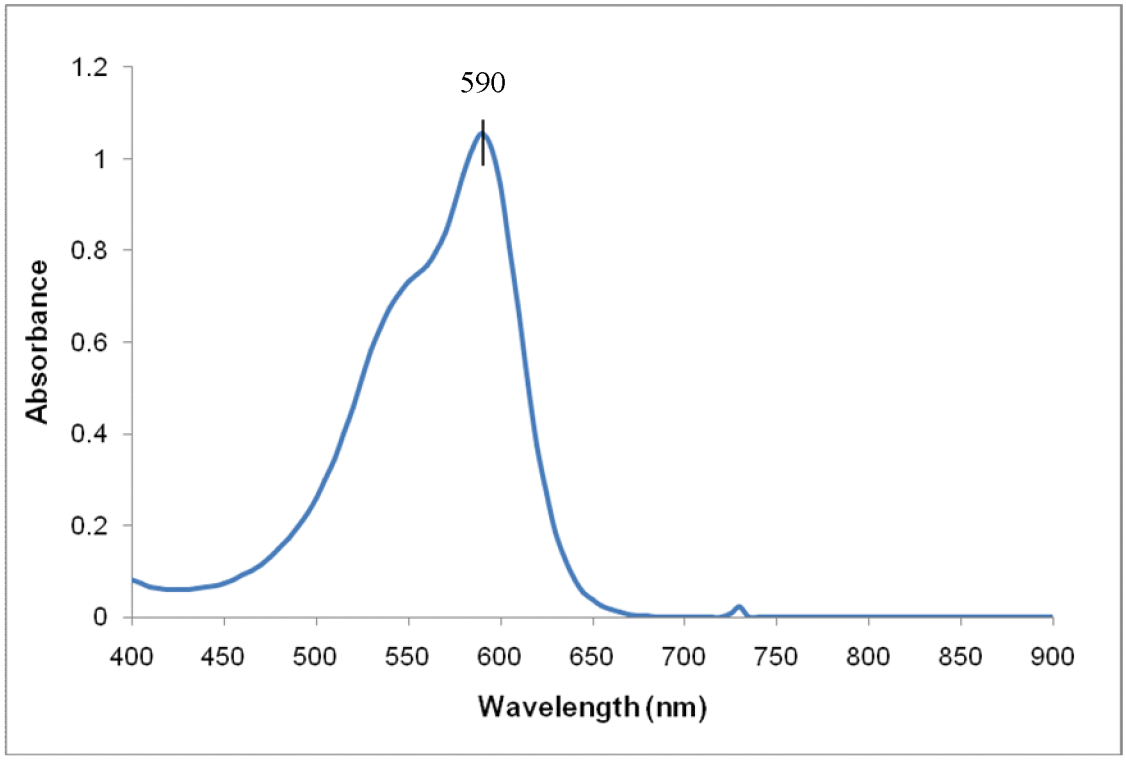

Figure 3.1: Crystal violet visible spectrum.

Crystal violet standard curve was prepared at A_{590nm} in order to estimate amount of dye remaining after the decolorization studies. The Crystal violet stock solution 60 ppm was prepared by adding 60 mg of Crystal violet into 1 L distilled water. Figure 3.2

showed the calibration plot for Crystal violet concentration ranging from 1 to 5 mg L^{-1}. Analysis was performed in triplicates.

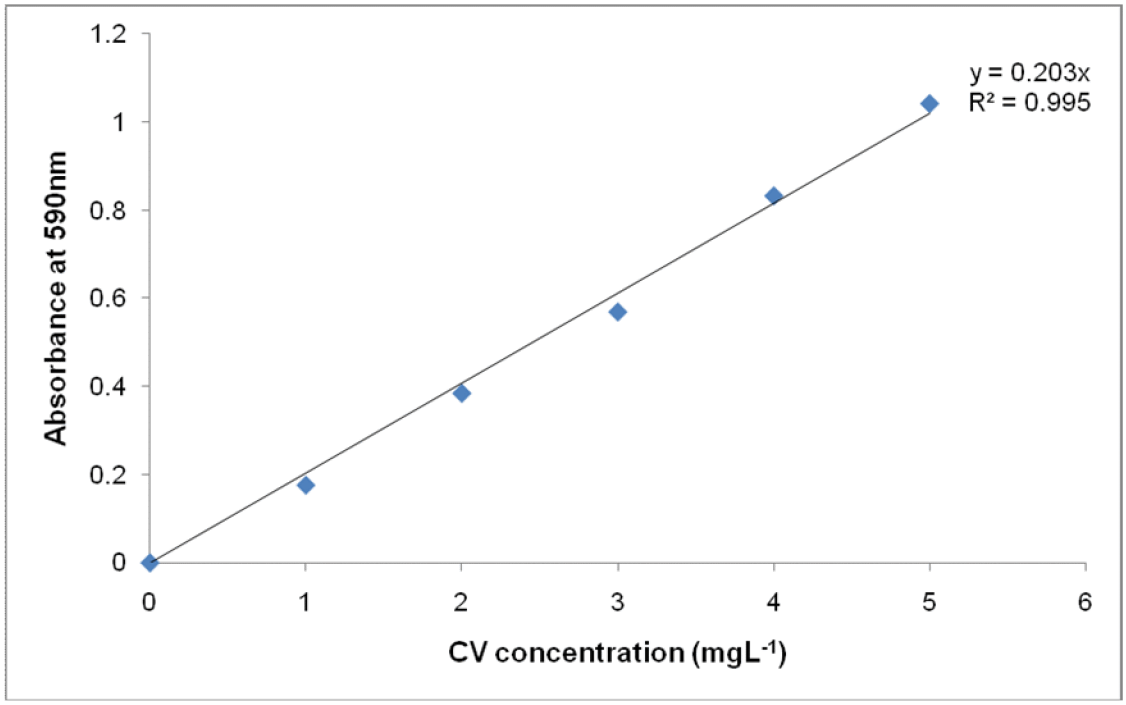

** Standard deviation of each data point < 0.5%. Each data point was an average of triplicate measurements.*

Figure 3.2: Standard calibration for Crystal violet.

3.4 Optimization of laccase immobilization parameters

Gel entrapment method was used in this study for the immobilization of laccase. Alginate solutions (2 and 3% w/v) were prepared by dissolving sodium alginate in distilled water. Alginate powder was added carefully to a well-stirred distilled water and stirring was continued until the solution was homogenous. Alginate solutions were mixed with 5 ml of laccase (0.6 U) at the alginate/laccase ratio of 1:1 and 8:5 (v/v) (Lu *et al.*, 2007). The mixture was stirred with magnetic stirrer to get a homogenous mixture. The mixture was then dripped into 20 ml of different $CaCl_2$ concentrations (2 and 3%, w/v)

using a 1 ml disposable syringe and left to harden for at least an hour under mild agitation to permit maximum reaction with Ca^{2+} ions (Maddhinni *et al.*, 2006). Beads were prepared following the combinations as shown in Table 3.2. Each set of combinations were run in triplicates.

Table 3.2: Optimization of laccase immobilization parameters.

Combination No.	Conc. of alginate solution (% w/v)	Ratio of alginate solution and enzyme solution (v/v)	Conc. of $CaCl_2$ solution (% w/v)
1	2	1:1	2
2	2	8:5	2
3	2	1:1	3
4	2	8:5	3
5	3	1:1	2
6	3	8:5	2
7	3	1:1	3
8	3	8:5	3

Consistent beads with diameter of 2.5 ± 0.5 mm were produced. The size and morphology of the beads were determined using Dino-Lite digital microscope (Taiwan). The beads were separated from the $CaCl_2$ solution using a small sieve. The filtrate was collected in a beaker. The beads were washed thoroughly with 30 ml distilled water and 10 ml of 50 mM phosphate buffer (pH 5) solution. The washing solutions were also collected in the same beaker. The beads were then transferred to another beaker containing 150 ml of 50 mM phosphate buffer (pH 5) solution.

3.4.1 Loading efficiency

The filtrate and the washings were subjected to protein assay to determine the amount of enzyme entrapped in the beads. Enzyme activity determination was also performed for the filtrate and washings. 3.0 ml of the filtrate plus washings solution was put in a cuvette and 0.2 ml of 0.1 mM syringadazine solution was added to it. The solution was mixed properly and then subjected to the time course measurement at 530 nm for 10 minutes. The initial rate of reaction was obtained and from the standard calibration plots for free laccase activity, the amount of enzyme in the filtrate plus washings can be determined. Three replicates were made for each method. All of these steps were performed to determine the loading efficiency of the beads. The enzyme remained in the beads were calculated by the following equation:

$$E_{rem} = E_{ini} - E_{fw} \qquad \text{Equation (9)}$$

where E_{rem} = the amount of enzyme retained in the beads after the immobilization process (μg)

E_{ini} = the initial amount of enzyme (μg)

E_{fw} = the amount of enzyme in the filtrate and washings (μg)

The loading efficiency was calculated using the following equation:

$$\text{Loading efficiency} = \frac{E_{rem}}{E_{ini}} * 100 \qquad \text{Equation (10)}$$

3.4.2 Immobilization efficiency

The activity of the immobilized enzyme was determined using syringaldazine as substrate. The beads were put in a beaker containing 150 ml buffer solution pH 5, 10 ml of 0.1 mM syringaldazine solution was added and the absorbance was recorded for every 5 minutes for 100 minutes. The absorbance data against time was recorded for each replicate. The average of the three replicates' absorbance was calculated and plotted against time for each combination.

The immobilization conditions which gave the highest value for both loading and immobilization efficiency were considered as optimum.

3.5 Protein estimation by the absorbance at 280 nm

Estimation of the protein content in the solutions was made by measuring their absorbance at 280 nm (Schmid, 2001). Phosphate buffer was used as blank and solvent for dilution of the samples. Absorption studies were carried out at 280 nm on a UV/Vis spectrophotometer Jasco V-630 (Japan). This procedure was carried out to double check the amount of residual enzyme left in the supernatant and washing solutions.

3.6 Design of experiment and statistical analysis

Combinations of selected process parameters (Crystal violet concentration, reaction time and agitation rate) were studied and optimized using RSM statistical experimental design (Box-Behnken). Since there are three factors (Table 3.2), each with three levels (minimum, middle and maximum point values), there are 45 experimental

runs including triplicates generated from MINITAB®14 (Table 3.3). The design was completely randomized along with the sampling. The means of three replicate values for all data in the experiments obtained were tested in a one-way analysis of variance (ANOVA) using MINITAB®14.

Table 3.3: The maximum, minimum and middle point values used in RSM to generate statistical combinations.

Parameter	**Value**		
	Minimum	**Middle point**	**Maximum**
Speed (rpm)	60	110	160
Dye Concentration (ppm)	5	17.5	30
Time (day)	1	2	3

Table 3.4: The combinations generated by MINITAB®14 software to determine the optimal dye concentration (ppm), time taken (day) and agitation speed (rpm).

Run Order	**Blocks**	**Speed (rpm)**	**Dye Concentration (ppm)**	**Time (day)**
1	1	160	30	2
2	1	160	30	2
3	1	110	30	3
4	1	110	17.5	2
5	1	60	30	2
6	1	110	17.5	2
7	1	160	5	2
8	1	110	30	1
9	1	110	30	3
10	1	60	17.5	3
11	1	110	5	3
12	1	110	17.5	2

13	1	160	17.5	1
14	1	60	17.5	1
15	1	110	5	3
16	1	60	17.5	3
17	1	160	5	2
18	1	110	17.5	2
19	1	110	17.5	2
20	1	60	17.5	1
21	1	160	30	2
22	1	110	5	1
23	1	60	5	2
24	1	160	17.5	1
25	1	110	30	1
26	1	110	5	1
27	1	110	17.5	2
28	1	160	5	2
29	1	60	30	2
30	1	60	17.5	1
31	1	60	17.5	3
32	1	160	17.5	3
33	1	60	30	2
34	1	160	17.5	3
35	1	160	17.5	3
36	1	110	5	3
37	1	110	30	3
38	1	110	17.5	2
39	1	160	17.5	1
40	1	110	30	1
41	1	110	17.5	2
42	1	60	5	2
43	1	110	17.5	2
44	1	110	5	1
45	1	60	5	2

Experiments were conducted to assess the optimum contact time (day) required for dye removal, initial dye concentration that is degradable by pre-determined amount of enzyme and agitation speed of the shaker.

3.7 Optimization of dye decolorization parameters

In this study, the ability of pure laccase from *T. Versicolor* was investigated to decolourize industrial triphenylmethane dye, Crystal violet. A series of conical flasks containing 100 ml of dye solution, 2 U of immobilized laccase/alginate beads were added and the reaction mixture was agitated using Daihan LabTech Shaker (Korea) according to the combinations design. Samples of the reaction mixture were collected at specified time to measure the residual dye absorbance. The percentage of effluent decolourization was calculated.

The residual dye concentration was measured spectrophotometrically at 590 nm and the dye decolorization was calculated according to the following equation:

$$\% = \frac{A_0 - A_f}{A_0} \times 100 \qquad \text{Equation (11)}$$

where % = percentage of decolorization

A_0 = the initial absorbance

A_f = the final absorbance

3.8 Stirred tank reactor experiments

Scaled up experiments were carried out in a 1.5 L cylindrical Perspex vessel to represent a stirred tank reactor (STR) (Figure 3.3). The impeller was positioned overhead on a centrally located stirrer shaft (Figure 3.4). The stirrer shaft was driven by IKA® Werke Eurostar Digital Mixer (Germany) at a pre-determined agitation speed. The total working volume used in this experiment was 1 L, a ten times increase in volume from the

shake-flask experiments. The amount of beads used was also proportionally increased in 10-folds from the shake-flask study.

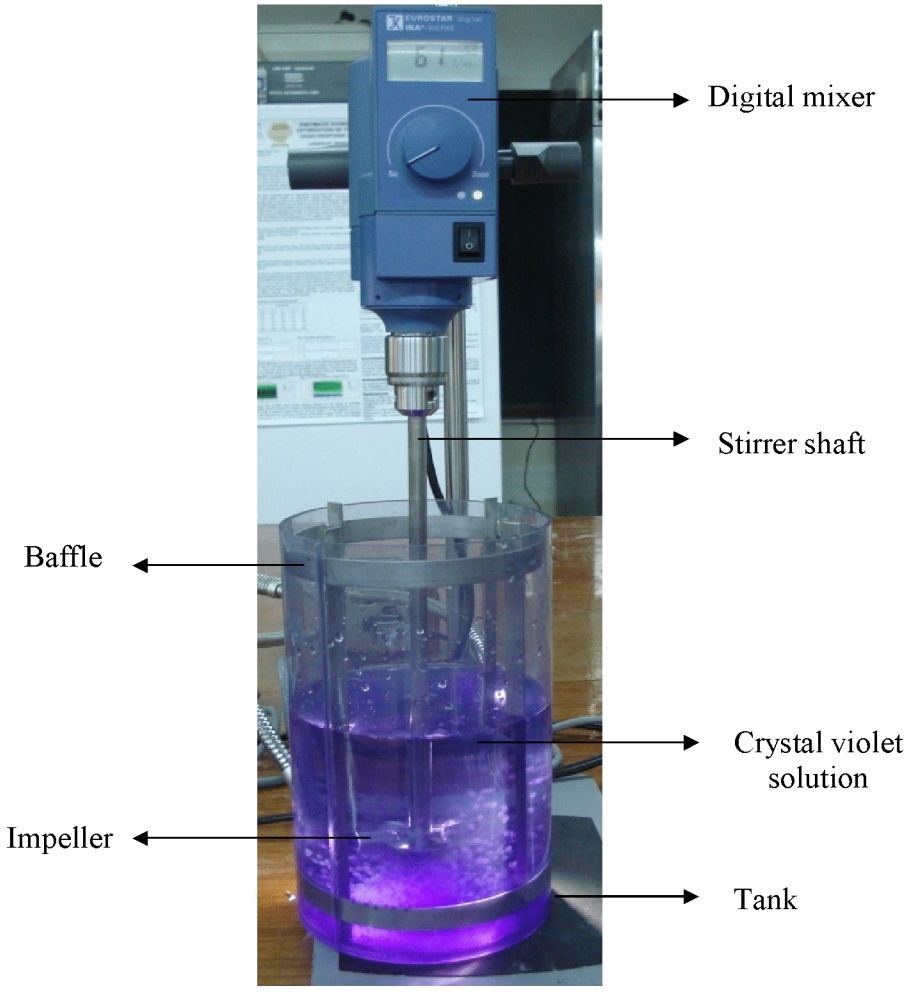

Figure 3.3: Stirred tank reactor (STR) experiments.

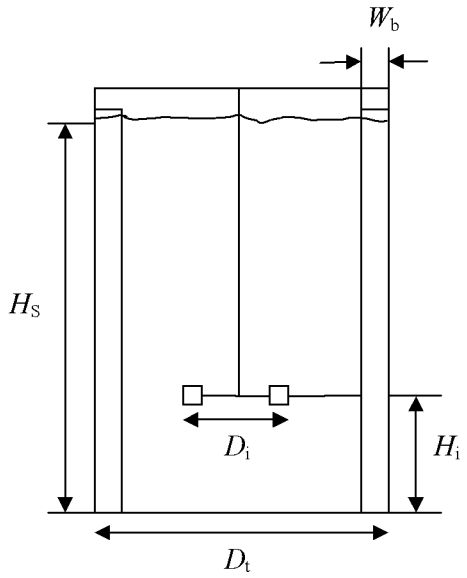

where D_t : Diameter of the tank (14.5 cm)

D_i : Diameter of the impeller (5 cm)

W_b : Width of the baffle (1.2 cm)

H_s : Height of the solution from the bottom of the tank (15 cm)

H_i : Height of the impeller from the bottom of the tank (5 cm)

Figure 3.4: Schematic diagram for stirred-tank reactor.

According to Doran (1995), the ratio of tank diameter (D_t) to impeller diameter (D_i) need to be about 3:1 for Newtonian fluid (*i.e.* Crystal violet solution in this case). For efficient mixing, the depth of liquid (H_s) in the tank should not be more than 1.0-1.25 times the tank diameter (D_t). Stainless steel baffles were installed to reduced central vortexing and swirling of the liquid. The baffle width (W_b) was about 10% of the tank

diameter (D_t). Table 3.5 shows the geometrical setup for mixing studies in the stirred tank reactor experiment.

Table 3.5: The ratio of diameter, heights and width for above specified configuration.

Impellers	D_t / D_i	H_s / D_i	H_s / D_t	H_i / D_i	Baffles	
					W_b / D_t	Number
60° angled blade and 180° curved blade impeller	3	3	1	1	0.8	4

3.8.1 Type of impellers used in STR experiment

Type of impellers used were:

1) 60° angled blade impeller (axial pumping down);
2) 180° curved blade impeller.

Figure 3.5: Types of impeller used in the stirred tank reactor experiment.

Figure 3.5 is a photograph of the impellers on the shaft. Figures 3.6 and 3.7 show the drawings of these impellers.

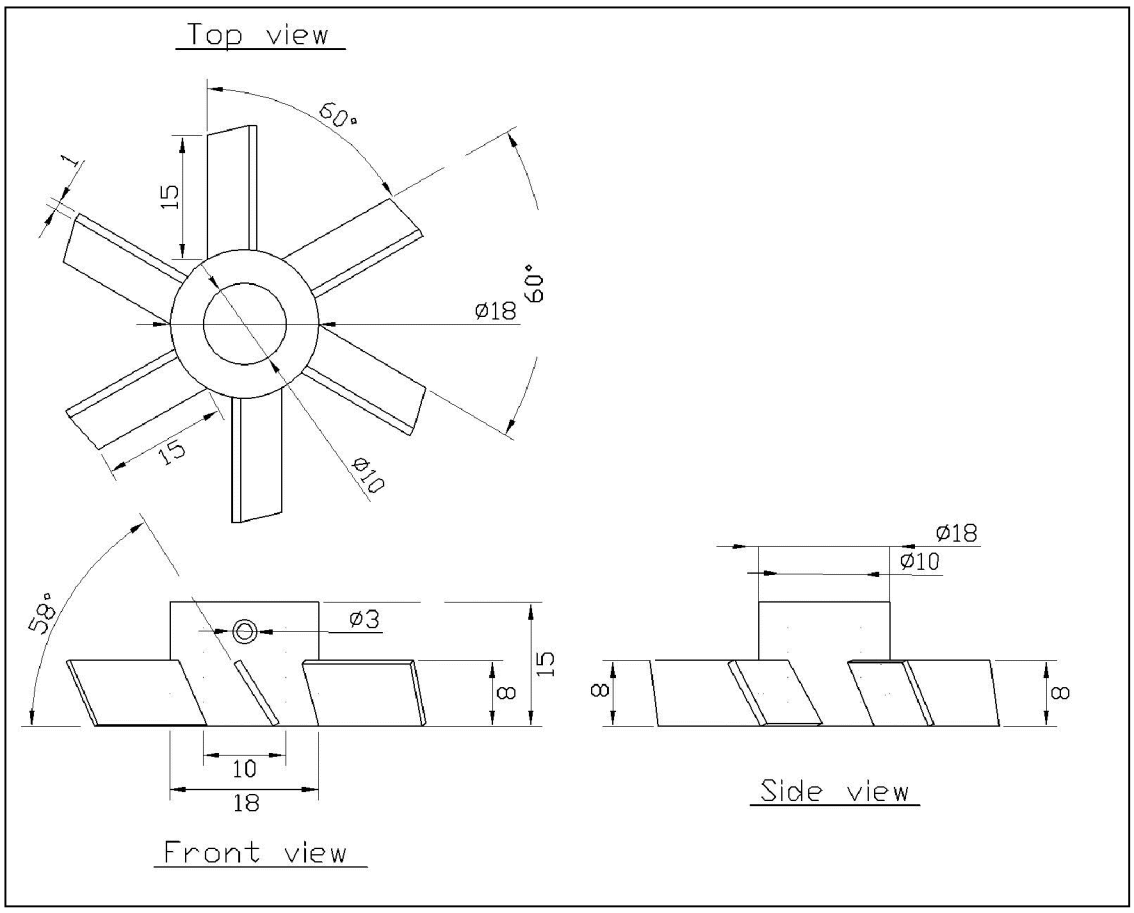

*All measurements are in mm.

Figure 3.6: Detail schematic 60° axial flat blade impeller (downward) from top, front and side view.

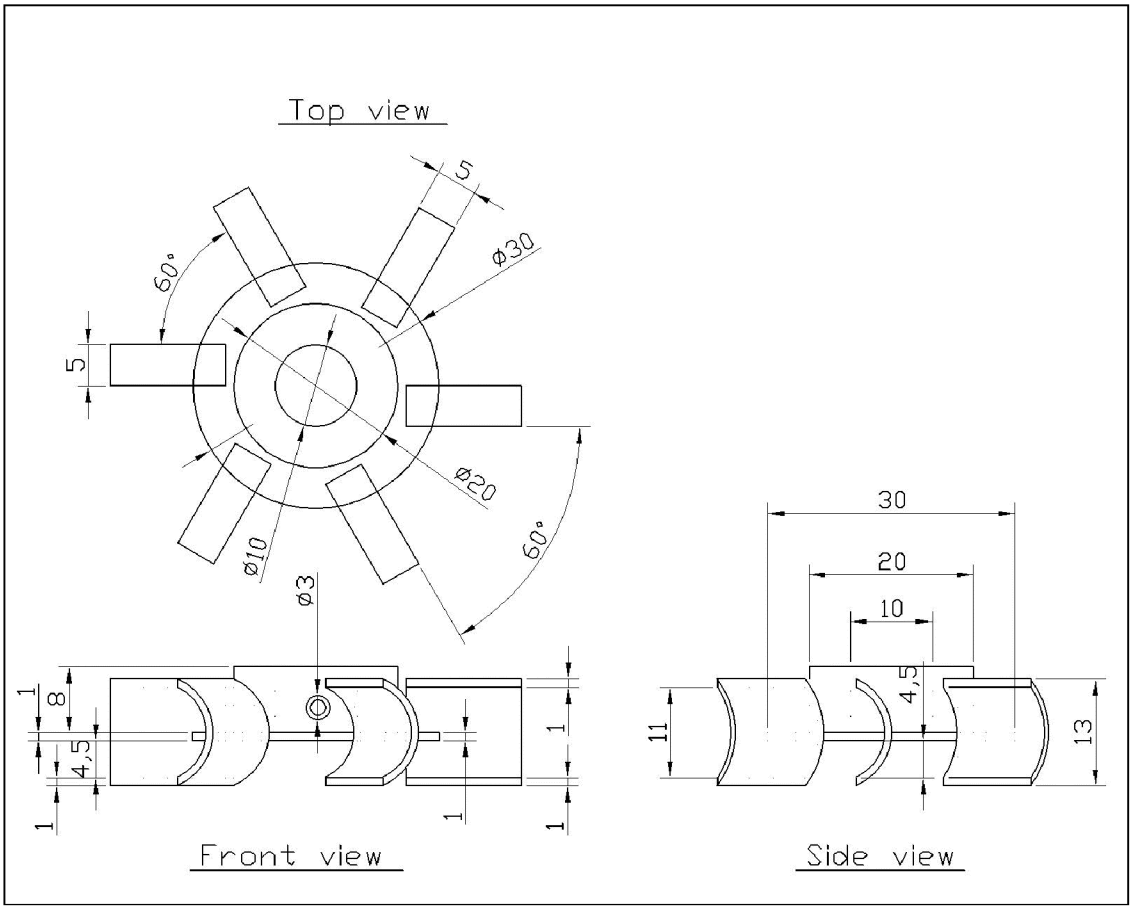

*All measurements are in mm.

Figure 3.7: Detail schematic 180° six curved blade impeller from top, front and side view.

Axial and radial flows are generated by the angled blade and curved blade impellers respectively and these motions are largely responsible for bulk mixing. Axial and radial flows are classified depending on the direction of liquid leaving the impeller. Axial flow impeller normally has blades that make an angle of less than 90° to the plane of rotation and promote axial top to bottom flow (Doran, 1995). Figure 3.8 illustrates the axial flow motion where fluid leaving the impeller was driven downwards until it was

deflected from the floor of tank. It then spread out over the floor and flowed up along the wall before being drawn back to the impeller.

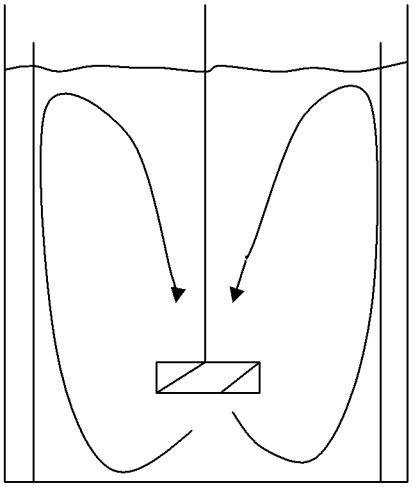

Figure 3.8: Flow pattern produced by a 60° axial flat blade impeller in a baffled tank.

In general, impellers that have blade parallel to the vertical axis of the stirrer shaft and tank will produce radial flow (Doran, 1995). The flow pattern produced by radial flow impeller was illustrated in Figure 3.9. Fluid was driven radially from the impeller against the walls of the tank where it divides into two streams, one flowing up to the top of the tank and the other flowing down to the bottom. These streams finally reached the central axis of the tank and are drawn back to the impeller. The curved blade impeller used in this study was observed to have this type of flow pattern.

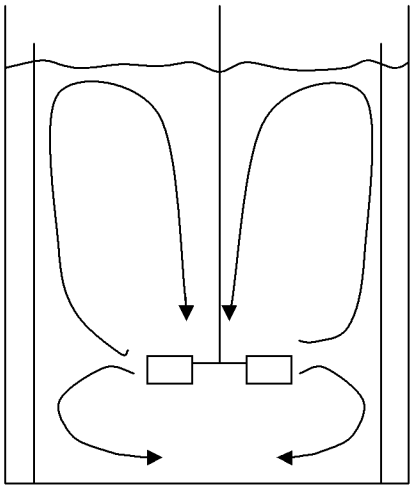

Figure 3.9: Flow pattern produced by a 180° curved blade impeller in a baffled tank.

Both of the impellers also produced simple circular flow around the shaft. This simple circular flow must be avoided because it created liquid flow in a streamline fashion and there is little mixing between fluids at different heights in the tank (Doran, 1995). This circular flow pattern can be reduced using baffles. The functions of installing baffle were to create turbulence in the liquid, interrupt circular flow pattern and avoid vortex at high speed where it can produced high mechanical stresses in the stirrer shaft, bearings and seal.

The effect of impeller geometries, initial dye concentrations (5 and 30 ppm) and rotational speed (60 and 160 rpm) towards dye decolorization were studied. The flow patterns for each blade were also analyzed in this research by looking at the movements of beads during the experiment.

3.8.2 Power requirements for ungassed Newtonian fluid in mixing

Power consumption by the axial and curved blade impellers were determined in this research using Equation (12).

$$N_P = \frac{P}{\rho N_i^3 D_i^5} \qquad \text{Equation (12)}$$

where N_P = power number

P = power (watt)

ρ = fluid density (kgm^{-3})

N_i = stirrer speed (rotational speed per second)

D_i = Impeller diameter (meter)

Power number used for 60° angled blade and 180° curved blade impellers are based on the work of Ibrahim & Nienow (1995) and Aziz (2007), which are 1.9 and 1.7 respectively for the angled blade and curved blade impellers. The properties of Crystal violet solution, namely the density and viscosity were presumed to be the same as water.

CHAPTER 4

RESULTS AND DISCUSSIONS

4.1 Determination of initial reaction rate of laccase using 0.1 mM syringaldazine as substrate

Five different laccase concentrations (0.005, 0.008, 0.01, 0.03 and 0.05 U) were used for linearity assay of laccase using 0.1 mM syringaldazine as substrate at 25 ± 1°C. Time course measurement data generated from the spectrophotometer for 10 minutes were shown in Figure 4.1.

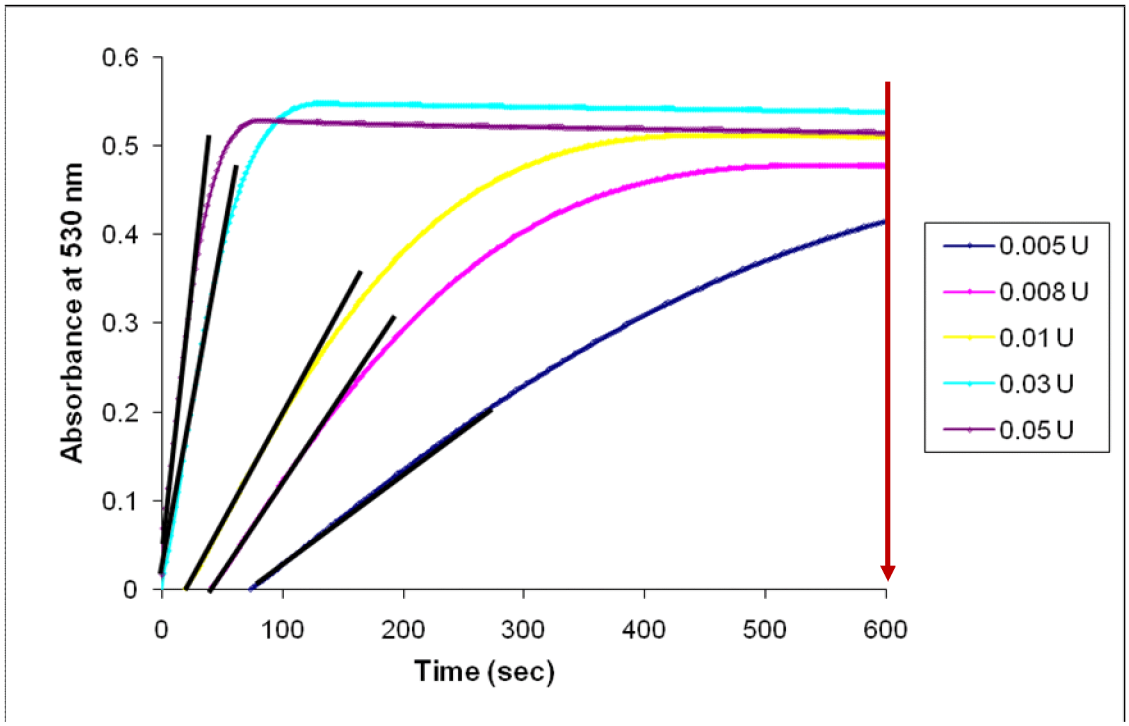

Figure 4.1: Laccase activity in 0.1 mM syringaldazine at 25 ± 1°C expressed in 3.4 ml of total reaction volume.

As the amount of laccase increases, the laccase activity increases correspondingly. For the highest amount of laccase tested, 0.05 and 0.03 U, the oxidation of syringaldazine occurred very rapidly from 0.8 to 1.6 minutes resulted in assay time which was too short. In contrast, enzyme concentration from 0.005 to 0.01 U required longer time (5 to 10 minutes) to oxidize syringaldazine which make it more practical to be used within this range of time. The equilibrium was reached after 10 minutes for all enzyme concentrations used. Hence, 10 minutes was used as the total assay time for laccase reaction in this study.

For each enzyme concentrations, the slope of absorbance curve against time (dA/dt) from Figure 4.1 was calculated and presented in Table 4.1. The initial rate of reaction can then be estimated using Equation (4). The Δt for the determination of dA/dt (slope) was fixed at approximately 10 seconds. From Table 4.1 it was clear that enzyme concentration was directly proportional to the initial rate of reaction. The calculated values for initial rate of reaction were then used to plot Figure 4.2. The purposed of this linearity assay was to estimate the initial rate of reaction of the enzyme as a function of enzyme concentration. Therefore, any enzyme concentration that was chosen within this range was expected to give the initial rate of reaction as predicted in Figure 4.2.

The percentage of product formation within 10 seconds was calculated using Equation (8). The assumption of initial rate of reaction was within 10 seconds, the product formation must be less or equal to 5% ($P \leq 5\%$) and the substrate must be more or equal than 95% ($S \geq 95\%$). This was done to make sure that there were high likelihood

of enzyme occupied by the substrate and give accurate estimation for the initial rate of reaction.

Table 4.1: Determination of initial rate of reaction for laccase using 0.1 mM syringaldazine as substrate.

Unit of Laccase (U)	**Initial rate of absorbance change per minute ($\Delta dA/\Delta dt$) or (v)**	**Initial rate of reaction (μmol min^{-1})**	**Percentage of product formation (%) in 10 seconds**
0.005	0.065	0.992 ± 0.07	0.17
0.008	0.122	1.871 ± 0.13	0.31
0.010	0.149	2.284 ± 0.11	0.38
0.030	0.489	7.523 ± 0.08	1.25
0.050	0.742	11.420 ± 0.12	1.90

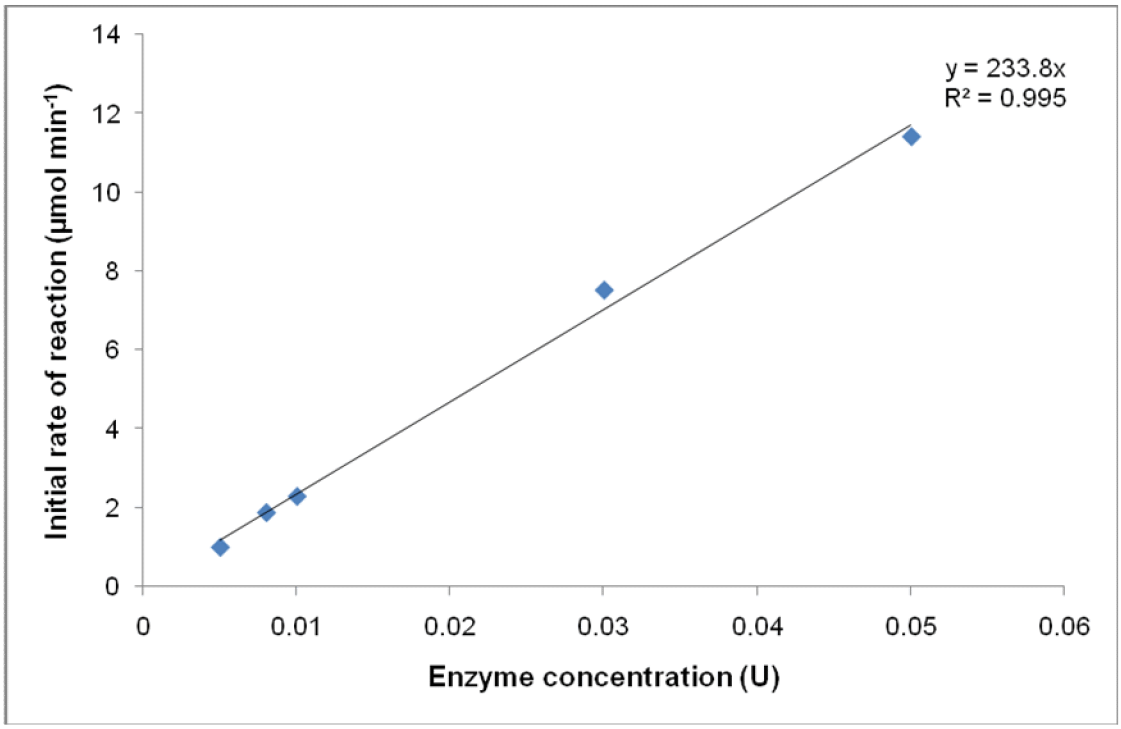

** Standard deviation of each data point < 0.5%. Each data point was an average of triplicate measurements.*

Figure 4.2: Initial rate of reaction for different units of laccase.

Figure 4.2 showed a linear relationship between the enzyme concentration and initial rate of reaction. With the R^2 value more than 0.99, it showed that it was a near perfect linear fitting which will allow good estimation of initial rate of reaction for the enzyme selected within this range (0.005 to 0.05 U). This plot was used for determination of free laccase activity in supernatant and washing solution during immobilization of enzyme in this study. By using this plot, the amount of enzyme left in the supernatant and washing solution can directly be determined using spectrophotometer analysis. Thus, by deducting the initial amount of laccase before immobilization and the total amount of enzyme left in supernatant and washing solution, the amount of enzyme immobilized inside the beads can be estimated.

4.2 Determination of kinetic parameters, K_m and V_{max} of free laccase using syringaldazine as substrate

The kinetics parameters, Michaelis-Menten constant (K_m) and maximum reaction rate (V_{max}) of laccase were determined using five different syringaldazine concentration (0.1, 0.2, 0.3, 0.4 and 0.5 mM) at 25 ± 1°C. The amount of laccase chosen in this assay was 0.03 U. This assay was performed in spectrophotometer and time course measurement data generated for 5 minutes were shown in Figure 4.3. The initial rate of reaction is directly proportional to the amount of substrate (syringaldazine). This was indicated by the increased of slope of absorbance curve against time.

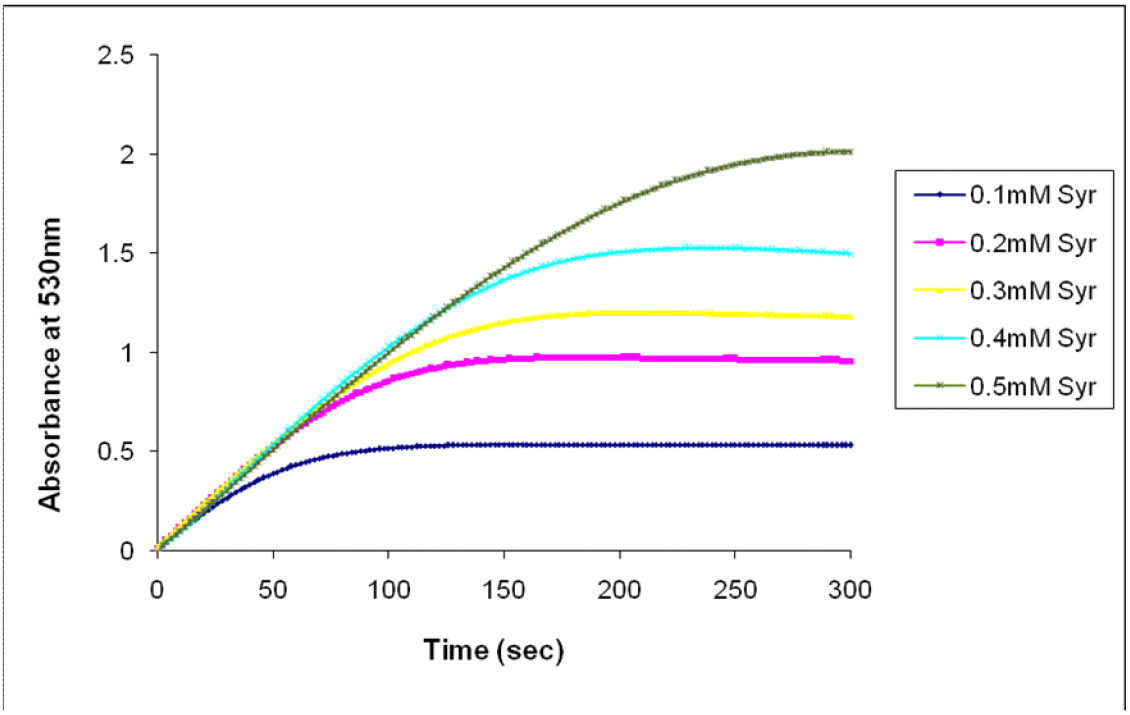

Figure 4.3: Laccase activity with different syringaldazine concentration expressed in total reaction volume of 3.4 ml.

For each substrate concentrations, the slope of absorbance curve against time (dA/dt) from Figure 4.3 was calculated and presented in Table 4.2. Then, the initial rate of reaction can be estimated using Equation (4). By plotting the initial rate of reaction against substrate concentration (syringaldazine), Figure 4.4 was obtained.

Table 4.2: Determination of initial reaction rate at different concentrations of syringaldazine as substrate.

Concentration of syringaldazine (mM)	**Initial rate of absorbance per minute (ΔAbs/ΔMin) or (v)**	**Initial rate of reaction (μmol min^{-1})**
0.1	0.537	8.259 ± 0.12
0.2	0.585	8.994 ± 0.14
0.3	0.600	9.239 ± 0.19
0.4	0.609	9.382 ± 0.03
0.5	0.614	9.448 ± 0.17

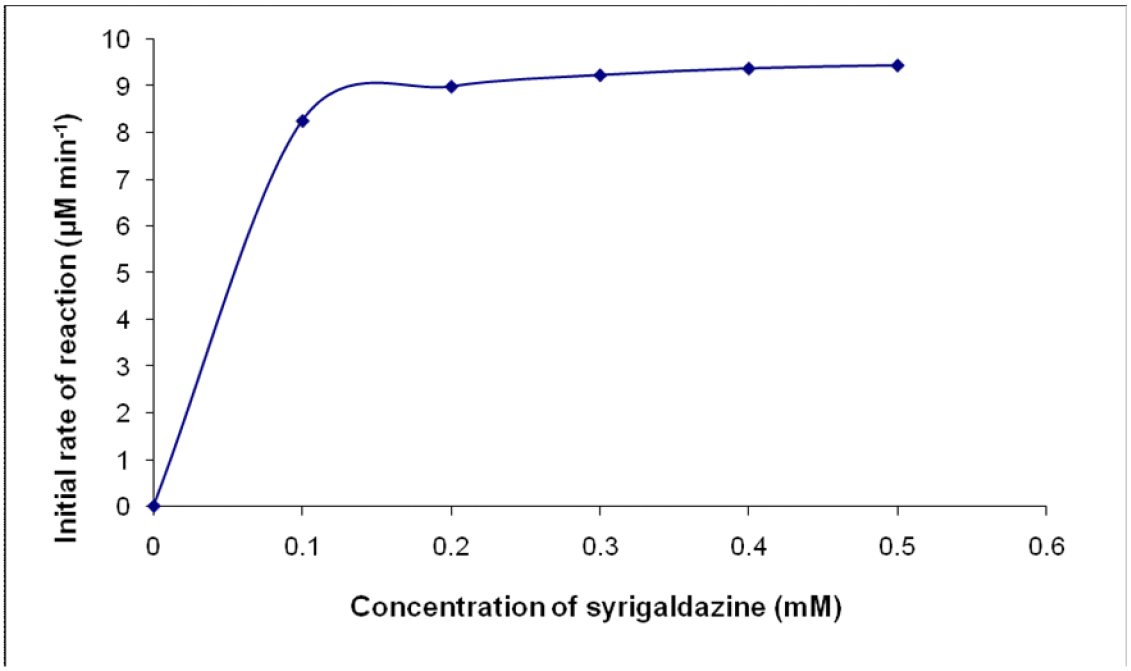

** Standard deviation of each data < 0.5%. Each data point was an average of triplicate measurements.*

Figure 4.4: Initial rate of reaction using different syringaldazine concentrations.

The initial rate of reaction was significantly increased from 0 to 0.1 mM of syringaldazine. From 0.2 to 0.5 mM syringaldazine, the rate of reaction slightly increased with the increase in subsrate (syringaldazine) concentration. This probably because the active site of the enzyme was saturated with the substrate and thus the oxidation activity was at the maximum. It was obvious from Figure 4.4 that the reaction rate profile appeared to follow the Michaelis-Menten kinetics. Subsequently, the K_m and V_{max} was determined using non-linear regression softwares; Lucenz (III) and Polymath® 6.0.

The V_{max} and K_m values estimation by the softwares were shown in Table 4.3.

Table 4.3: Calculated V_{max} and K_m values from Lucenz (III) and Polymath® 6.0 softwares.

Kinetic parameters	Software	
	Lucenz (III) software	**Polymath® 6.0**
V_{max}	9.82 ± 0.001 μM min^{-1}	9.82 ± 0.03 μM min^{-1}
K_m	0.0188 ± 0.001 mM	0.0187 ± 0.0008 mM

The Lucenz (III) and Polymath® 6.0 software were used to perform non-linear regression in evaluation of both K_m and V_{max}. Table 4.3 showed the results obtained from these softwares. The V_{max} and K_m values obtained from both softwares were approximately the same. The V_{max} and K_m for Lucenz (III) and Polymath® 6.0 were 9.82 ± 0.001 μM min^{-1}, 9.82 ± 0.03 μM min^{-1}, 0.0188 ± 0.001 mM and 0.0187 ± 0.0008 mM respectively. From the K_m value obtained, the use of 0.1 mM syringaldazine to assay enzyme activity throughout the study was justified, as this concentration was 10-fold higher than the K_m. This increases the likelihood that almost the enzyme molecules were occupied by the substrate for reaction.

4.3 Calcium alginate entrapment profile to determine the optimum immobilization condition

Calcium alginate entrapment method was chosen to immobilize laccase because this method can be performed in extremely mild conditions, which the gelation of calcium alginate does not depend on the formation of permanent covalent bond, but the

alginate molecules are cross-liked by calcium ions (Park *et al.*, 1995 and Nilsson, 1987). The amount of calcium ions and alginate used need to be determined in this research since the alginate beads were formed by combinations of these two components. Other factor tested was volume ratio between alginate and laccase solution. The loading efficiency was defined as the percentage of total enzyme entrapped in the calcium-alginate beads. Table 4.4 showed the percentage of loading efficiency for eight different combinations. From the results shown, it can be concluded that loading efficiency was above 90% for all concentrations chosen. Although the loading efficiency for all of the combinations was above 90%, the immobilized enzyme activity was then assessed to determine the most optimum immobilization condition (Figure 4.5).

Table 4.4: Percentage of loading efficiency in different configuration of alginate beads.

Combination No.	Conc. of alginate sol. (% w/v)	Ratio of alginate sol. and enzyme sol. (v/v)	Conc. of $CaCl_2$ sol. (% w/v)	Actual amount of protein used (µg)	Protein lost in filtrate + washings (µg)	Activity in filtrate + washings (µmol min^{-1})
1	2	1:1	2	750	53	Not detected
2	2	8:5	2	750	63	Not detected
3	2	1:1	3	750	48	Not detected
4	2	8:5	3	750	51	Not deetcted
5	3	1:1	2	750	67	0.0004
6	3	8:5	2	750	59	Not detected
7	3	1:1	3	750	62	0.0012
8	3	8:5	3	750	49	Not detected

Lu *et al.* (2007) reported, beads that were prepared using lower alginate and $CaCl_2$ concentration (1% w/v) showed a lower immobilization yield. Won *et al.* (2005) suggested this probably because of the weak cross-linking and loose structure of the beads prepared, hence, promotes enzyme leakage. For this reason, the optimal parameters need to be selected in such a way that a reasonable amount of immobilization efficiency is maintained. Therefore, it this study, higher alginate and $CaCl_2$ concentrations of 2 and 3% w/v were chosen. Generally, an increase in alginate and calcium ion concentration would lead to formation of beads with more compact and rigid matrices, thus, enzyme leakage would be minimized. Nevertheless, the beads prepared at the highest concentration of alginate and $CaCl_2$ did not showed high immobilized yield as expected. This can be clearly seen in Figure 4.5, where the 3% w/v of alginate and $CaCl_2$ showed lowest enzyme activity and increased lag time. Lu *et al.* (2007) and Won *et al.* (2005) suggested that compact and rigid structure of beads would decrease enzyme flexibility and substrate diffusion, subsequently leading to low activity of immobilized enzyme.

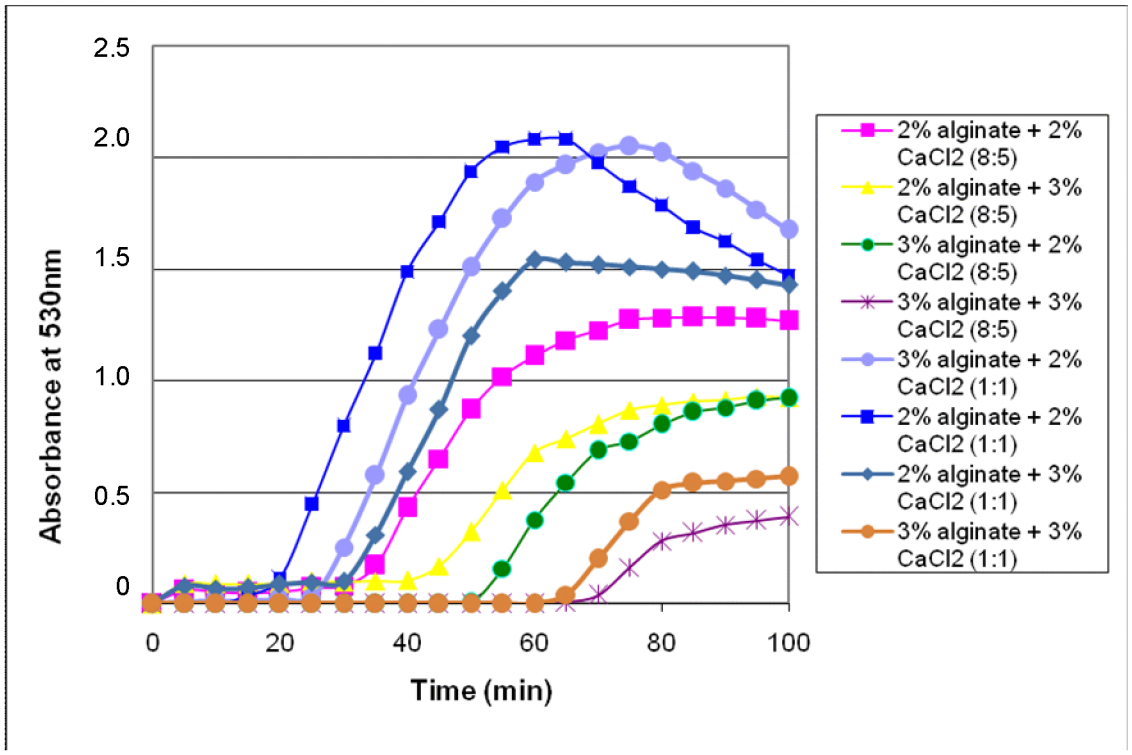

Figure 4.5: Different beads configuration to determine the best condition for immobilized laccase.

High volume of alginate to laccase ratio (8:5) decreased the immobilized yield. This due to more rigid beads produced by high volume of alginate. In particular, beads prepared at the 1:1 ratio of alginate to enzyme showed the highest immobilized enzyme activity yield. For a consistent bead formation, the ratio of volumes of sodium alginate and enzyme solution was maintained at 1:1.

From Figure 4.5, it was evident that the combination of lower calcium chloride and alginate concentration reduced the lag time. The lag time is the time required for the substrate to cross the barrier of the beads. Calcium alginate matrix and liquid-film layer around the beads formed significant barriers for substrate to enter the bead. Minimum lag

time around 20 minutes was observed within beads with less rigid structure. However, more compact and solid beads showed increased lag time from 40 minutes to 1 hour as the time required by the substrate to diffuse through will also increase. Overall, enzyme activity decreased with higher concentration of alginate and $CaCl_2$.

The combination with least lag time and highest immobilized enzyme activity yield was considered optimum condition for immobilization of laccase. Based on above results, the optimum parameters for enzyme immobilization were found to be 2% w/v calcium chloride solution, 2% w/v alginate solution and 1:1 ratio of alginate to enzyme solution with small lag time (20 minutes) and highest immobilized activity yield.

4.4 Calcium alginate beads morphology

From Figure 4.6, the left panel indicated the freshly prepared beads and the right panel showed absorption of crystal violet into the beads. Crystal violet need to be absorbed into the beads in order to react with laccase, which were immobilized inside the beads. Calcium alginate beads that produced were in diameter ranging from 2.5 ± 0.5 mm. Lu *et al.* (2007) and Won *et al.* (2005) reported that the activity of immobilized enzyme increased with decreasing beads size due to less mass transfer resistance. In addition, the small beads will have better ability absorption due to the increased surface/volume ratio. Hence, enzyme immobilized in small alginate beads will have advantages in toxic effluent treatment.

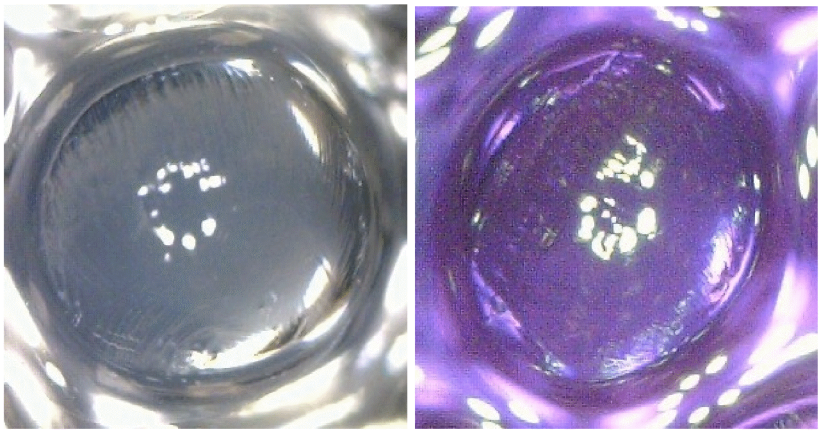

Figure 4.6: Calcium alginate beads.

4.5 Selection of the best parameter combination and statistical analysis

In this study, the Box–Behnken experimental design was chosen for finding out the relationship between the response function (percentage of decolorization) and variables (dye concentration, process time and agitation speed). The results of the 45 experimental runs including replicates based on MINITAB®14 design were tabulated in Table 4.5 below.

Table 4.5: Box-Behnken experimental results for 45 runs at three variables: agitation speed (rpm), dye concentration (ppm) and process time (day).

Run Order	Blocks	Speed (rpm)	Dye Concentration (ppm)	Time (day)	Percentage of Decolorization (%)
1	1	160	30	2	30.6
2	1	160	30	2	32.5
3	1	110	30	3	26.1
4	1	110	17.5	2	38.9
5	1	60	30	2	27.6
6	1	110	17.5	2	30.5
7	1	160	5	2	40.1
8	1	110	30	1	25.6

9	1	110	30	3	27.1
10	1	60	17.5	3	25.1
11	1	110	5	3	30.4
12	1	110	17.5	2	27.9
13	1	160	17.5	1	25.4
14	1	60	17.5	1	25.0
15	1	110	5	3	36.9
16	1	60	17.5	3	25.2
17	1	160	5	2	40.1
18	1	110	17.5	2	32.8
19	1	110	17.5	2	33.8
20	1	60	17.5	1	27.9
21	1	160	30	2	30.8
22	1	110	5	1	30.5
23	1	60	5	2	35.4
24	1	160	17.5	1	30.2
25	1	110	30	1	25.0
26	1	110	5	1	34.9
27	1	110	17.5	2	34.2
28	1	160	5	2	39.2
29	1	60	30	2	30.1
30	1	60	17.5	1	24.3
31	1	60	17.5	3	27.9
32	1	160	17.5	3	33.4
33	1	60	30	2	29.0
34	1	160	17.5	3	31.7
35	1	160	17.5	3	32.9
36	1	110	5	3	35.1
37	1	110	30	3	28.9
38	1	110	17.5	2	34.9
39	1	160	17.5	1	29.7
40	1	110	30	1	27.2
41	1	110	17.5	2	27.1
42	1	60	5	2	35.5
43	1	110	17.5	2	39.7
44	1	110	5	1	32.4
45	1	60	5	2	33.4

Data from Table 4.5 was then used to determine regression coefficient (Table 4.6 and Table 4.8) and analysis of variance (ANOVA - Table 4.7 and Table 4.9) for full quadratic model and model comprising of linear and square effects only.

Table 4.6: Full quadratic of estimated regression coefficients, *T*-value and *P*-value for percentage of decolorization (%).

Term	**Coefficient**	**Standard Error Coefficient**	***T***	***P***
Constant	14.9570	6.69014	2.236	0.032
Speed	0.0843	0.07739	1.089	0.284
Dye Conc. (mg/l)	-0.3967	0.24958	-1.589	0.121
Day	16.3838	3.66667	4.468	0.000
Speed*Speed	-0.0003	0.00031	-0.917	0.366
Dye Conc. (mg/l)*Dye Conc. (mg/l)	0.0069	0.00492	1.399	0.171
Day*Day	-4.3857	0.76894	-5.704	0.000
Speed*Dye Conc. (mg/l)	-0.0011	0.00118	-0.911	0.369
Speed*Day	0.0193	0.01478	1.306	0.200
Dye Conc. (mg/l)*Day	-0.0017	0.05910	-0.028	0.977

$S = 2.559$ $R^2 = 74.5\%$ $R^2(adjusted) = 68.0\%$

From Table 4.6 above, the main effects and interactive terms which have *P*-value less than 0.05 (*P*-value < 0.05) is considered significant whereas the *P*-value greater than

0.05 (P-value > 0.05) is considered to be insignificant in this study. Process time (day) was highly significant where the value of P was <0.05. The interactive term between day*day (P = 0.000) was the only combination that was significant in this full quadratic model.

The sign of the coefficients demonstrated the performance of the response i.e. when the factor has a positive effect, it indicates the response is higher at the high level and when the factor has a negative effect, the response is lower at high level (Haaland, 1989). The fully second-order model was described in Equation (13). The regression coefficient (R^2) and adjusted regression coefficient (R^2*(adjusted)*) are usually used to check the fit of the model and explain the model. R^2 particularly is a correlation coefficient to compare the model and experimental data. On the other hand, R^2*(adjusted)* is a correlation coefficient to compare the current model with other possible models. The higher its value, the better the model in explaining the experimental data. This model showed of R^2 and R^2*(adjusted)* values of 74.5 % and 68.0 %, respectively. In addition, the experiments showed a low value of errors term, S (2.559).

$$y = 14.9570 + 0.0843X_1 - 0.3967X_2 + 16.3838X_3 - 0.0003X_1^2 + 0.0069X_2^2 - 4.3857X_3^2 - 0.0011X_1X_2 + 0.0193X_1X_3 - 0.0017X_2X_3 \quad \text{Equation (13)}$$

where y = the model output *i.e.* percentage of decolorization (%)

X_1 = speed

X_2 = dye concentration

X_3 = day

The full quadratic second-order polynomial model in Equation (13) needs to be reduced since the interaction term in this model was statistically insignificant at the 5% level. Therefore, the new equation for percentage of crystal violet was proposed (Equation 14). Since both of the equations were an estimated equation and not a theoretical, therefore the error term was not included in these equations (Haaland, 1989).

Table 4.7: Full quadratic analysis of variance (ANOVA) for percentage of decolorization (%).

Source	**DF**	**Seq SS**	**Adj SS**	**Adj MS**	***F***	***P***
Regression	9	669.934	669.934	74.4371	11.37	0.000
Linear	3	415.566	170.607	56.8691	8.68	0.000
Square	3	237.763	237.763	79.2545	12.10	0.000
Interaction	3	16.604	16.604	5.5348	0.85	0.479
Residual Error	35	229.229	229.229	6.5494		
Lack-of-Fit	3	2.469	2.469	0.8231	0.12	0.950
Pure Error	32	226.759	226.759	7.0862		
Total	44	899.163				

where DF = degrees of freedom

Seq SS = sequential sum of squares

Adj SS = adjusted sum of squares

Adj MS = adjusted mean of squares

Based on the Table 4.7, the ANOVA for percentage of decolorization was shown to be highly significant for linear and square terms since the *P*-values of linear and square were < 0.05. The interaction effect was insignificant since the *P*-value was 0.479. This means only linear and square terms were important in the regression model. Since the interaction term was insignificant in this study, this term was discarded and new reduced second order model containing only linear and square terms were generated (Table 4.8 and 4.9). The lack of fit for this model was not significant as the *P*-value was 0.950.

Table 4.8: Linear and square of estimated regression coefficients, *T*-value and *P*-value for percentage of decolorization (%).

Term	**Coefficient**	**Standard Error Coefficient**	***T***	***P***
Constant	12.8437	4.94294	2.598	0.013
Speed	0.1040	0.06805	1.529	0.135
Dye Conc. (ppm)	-0.5184	0.17615	-2.943	0.006
Day	18.4766	3.10066	5.959	0.000
Speed*Speed	-0.0003	0.00031	-0.922	0.362
Dye Conc. (ppm)*Dye Conc. (ppm)	0.0069	0.00489	1.408	0.167
Day*Day	-4.3857	0.76422	-5.739	0.000

$S = 2.543$ $R^2 = 72.7\%$ $R^2(adjusted) = 68.3\%$

The new reduced regression model (Table 4.8) showed, the main effects and interaction between terms such as dye concentration (P = 0.006), day (P = 0.000) and day*day (P = 0.000) were highly significant where the P-value < 0.05 at 95% confidence level. However, for main effect speed (P = 0.135) and interactions between speed*speed (P = 362) and dye concentration*dye concentration (P = 0.167) were insignificant as the P-value > 0.05. This indicates that speed has no significant effect on optimization process in this study. Although the agitation factor was statistically insignificant within the range tested in this study, it was maintained in the model because agitation plays an important role in mixing to get a homogenous solution mixture (Doran, 1995). However, this condition has industrial advantages as the lowest speed can be employed in dye decolorization process. It will reduce the operational cost and at the same time retains the practicality of decolorization process. Hence, the lowest speed at 60 rpm was chosen for optimization program.

The significant effect shown by process time (day) on optimization was probably due to time required for crystal violet to diffuse inside alginate beads to be able to react with laccase. Dye concentration was important in the optimization process as rate of decolorization increases with the dye concentration being used. When all laccase molecules are complexed with substrate (crystal violet), further increase in substrate concentration will have no significant effect on the rate of reaction.

In addition, the high values of regression coefficient, R^2 and adjusted regression coefficient R^2*(adjusted)* 72.7% and 68.3% respectively showed that this model

can be used to explain most of the variations in the data. This is supported by low value of error terms, S (2.543).

A second-order regression model was then used to express the results obtained above. The regression model as given by the MINITAB®14 is stated below:

$$y = 12.8437 + 0.1040X_1 - 0.5184X_2 + 18.4766X_3 - 0.0003X_1^2 + 0.0069X_2^2 - 4.3857X_3^2$$

(Equation 14)

where y = the model output *i.e.* percentage of decolorization (%)

X_1 = speed

X_2 = dye concentration

X_3 = day

The result of analysis of variance (ANOVA) was tabulated in Table 4.9.

Table 4.9: Linear and square analysis of variance (ANOVA) for percentage of dye decolorization (%).

Source	**DF**	**Seq SS**	**Adj SS**	**Adj MS**	***F***	***P***
Regression	6	653.330	653.330	108.888	16.83	0.000
Linear	3	415.566	315.429	105.143	16.25	0.000
Square	3	237.763	237.763	79.254	12.25	0.000
Residual Error	38	245.833	245.833	6.469		
Lack-of-Fit	6	19.074	19.074	3.179	0.45	0.840

Pure Error	32	226.759	226.759	7.086
Total	44	899.163		

where DF = degrees of freedom

Seq SS = sequential sum of squares

Adj SS = adjusted sum of squares

Adj MS = adjusted mean of squares

Based on Table 4.9, the ANOVA for percentage of decolorization showed significant statistical values for linear and square effects at *F*-values equal to 16.25 and 12.25 respectively, and *P*-value < 0.05 for both. This indicates that the linear and square terms were important in the reduced regression model. Furthermore, the lack of fit was insignificant (> 0.05) and this specified that this model was well fitted with the experimental data. Statistical plots for analyses of experimental data were also constructed.

4.5.1 RSM normality test for percentage of decolorization

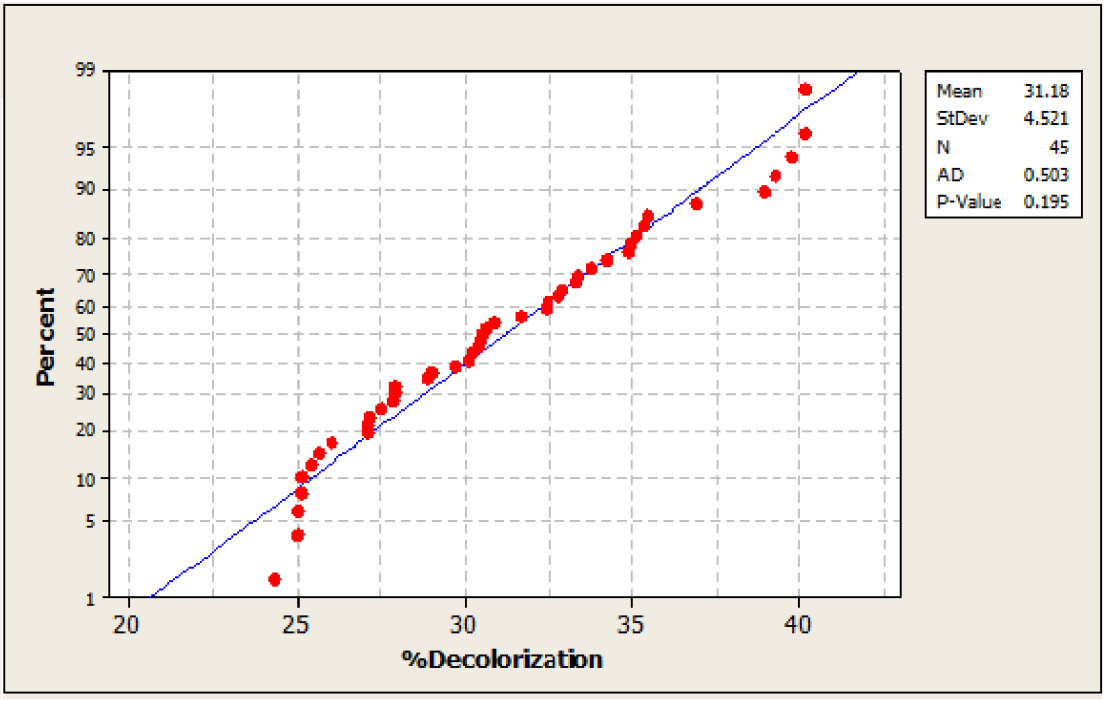

Figure 4.7: Normal probability plot of the results.

The normal probability plot is used to determine how well the data follow a normal distribution. The normal probability plot for the results (Figure 4.7) showed that the experimental data collected followed a normal distribution. The degree of fit is indicated by the degree to which the data points follow the fitted straight blue line. The small value (0.503) of goodness-of-fit test i.e. Anderson Darling statistic (AD) indicates that the distribution fits the data well. AD statistic is a squared distance that is weighted more heavily in the tails of the distribution. Hence, the smaller the AD values the distribution fits the data better. This plot also showed the *P*-value to be 0.195 at 5% significance level. This indicated that the deviation of data from normal assumption is not significant.

4.5.2 RSM residual plots for percentage of decolorization

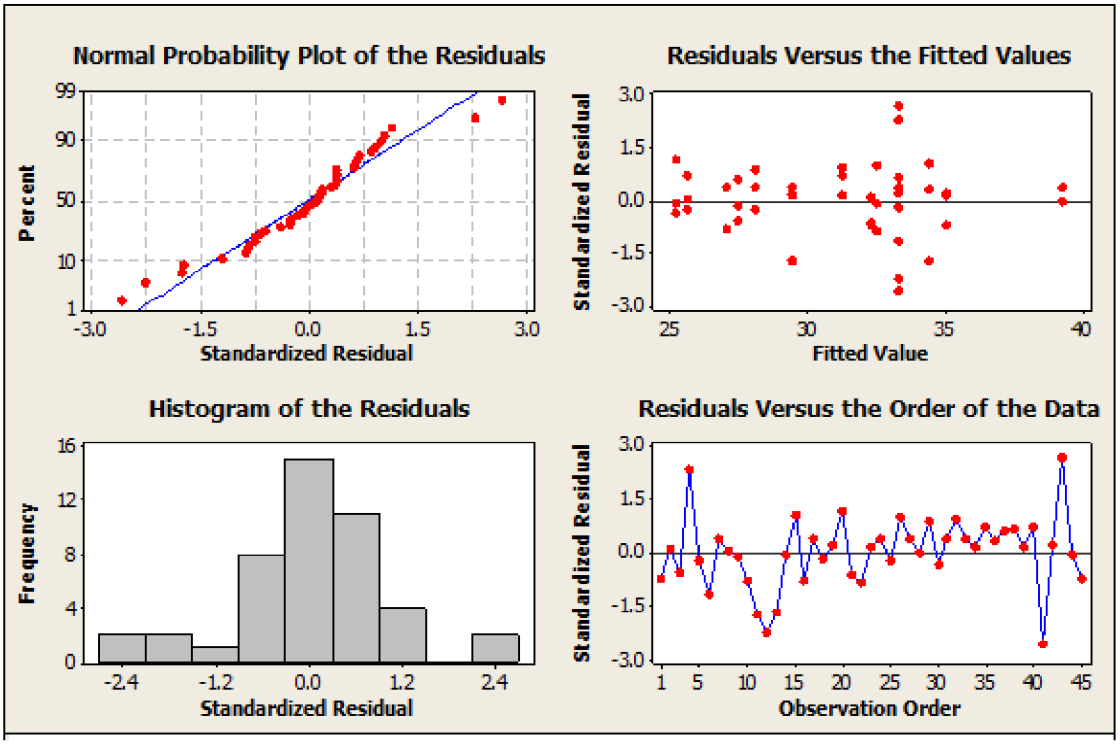

Figure 4.8: Residual plots for the results.

Figure 4.8 showed four different graphs for residual analyses. Residual values are derived from experimental values deducted by the model fitted values (Residuals = Experimental values – Model fitted values). The normal probability plot of residuals (top left panel) showed that the residuals were normally distributed. As the data fewer than 50 observations, the plot displayed curvature in the tails even if the residuals are normally distributed (Segel, 1975). This normal probability assumption was supported by the bell-shape curve of the histogram (bottom left panel) although one of the bars is quite far from the others which was due to outliers. This indicates that the error generated from the experimental data collected were solely due to random error. By observing the residuals against fitted (predicted) value graph (top right panel), a random pattern of residuals on

both sides of standardized zero line indicated the absence of systematic errors in the experiment. The order of collecting data has no influence on the data collected as shown by the lack of strong pattern in standardized residuals versus the observation order (bottom left panel) graph. Overall, it can be concluded that the pattern of residual data were normally distributed and were less likely influenced by non-random and systematic errors.

4.5.3 RSM main effects plot for percentage of decolorization

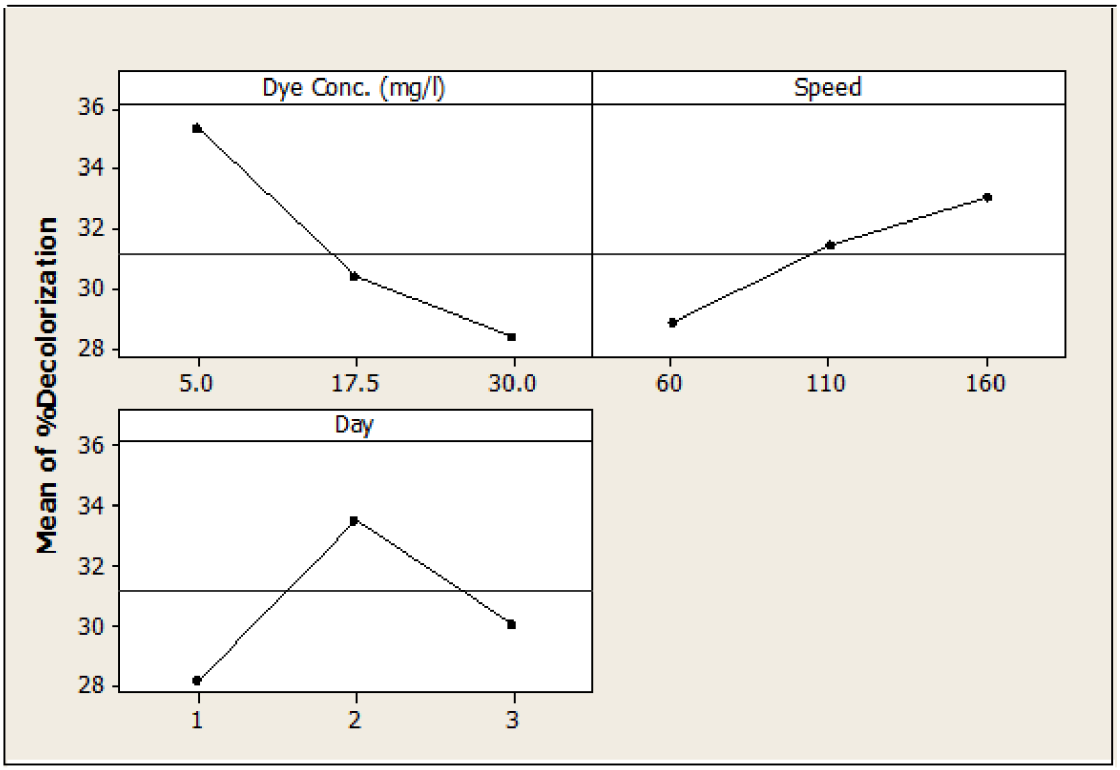

Figure 4.9: Main effects plot.

Figure 4.9 represents the change in the response i.e. percentage of crystal violet decolorization after reaction with laccase with respect to dye concentration (mg L^{-}

[1]), process time (day) and agitation speed (ppm) variables. Based on this graph, the steeper the line, the stronger the parameter effect on the response. It could be seen that as these three variables were varied, the response also changed. It was evident that the agitation speed has minimal effect on dye decolorization within the selected range of values since it has least steep line with the response (29 to 32%). Conversely, dye concentration and process time (day) have steepest lines that indicate strong effect as the responses were distributed within a relatively broad range (36 to 30% for dye concentration and 28 to 34% for day). The positive gradient shows that at a higher level of the main effects, the percentage of decolorization increasing and *vice versa*. Table 4.6 supported the results from Figure 4.9 where the *P*-value for dye concentration and day were < 0.05 while the agitation speed was the least significant with *P*-value > 0.05. In process time (day) plot, it indicated the percentage of decolorization was increased from 1 to 2 days but when it reached 3 days, there was a decline in the decolorization of crystal violet. This indicated that, the optimum day for decolorization could be at day 2. The main effect plot for dye concentration demonstrates that the lowest initial dye concentration employed would result in high percentage of decolorization. However, at higher dye concentration, the percentage of decolorization decreases. This probably due to non-competitive inhibition of the enzyme at high dye concentrations (Glanville & Clark, 1997). Although agitation speed was deemed to be insignificant from the statistical analyses, it is apparent that within the range tested, a slight increase in dye decolorization could still be observed at higher speed. The main effects plot could be used to provide general direction for the optimization of crystal violet decolorization *viz.* 5 ppm initial dye concentration, 160 rpm agitation speed and 2 days process time. The possible

interactions between the parameters were then examined using contour plots as shown in the Figure 4.10, 4.11 and 4.12.

4.5.4 RSM counter plots for percentage of decolorization

Contour plots were constructed using MINITAB®14 to evaluate the response (*i.e.* percentage of decolorization) when two different parameters were varied simultaneously while keeping another parameter at their respective middle level. Three contour plots of calculated responses from the interaction between agitation speed and process time (day), initial dye concentration and process time (day), initial dye concentration and agitation speed are illustrated in Figure 4.10, 4.11 and 4.12, respectively.

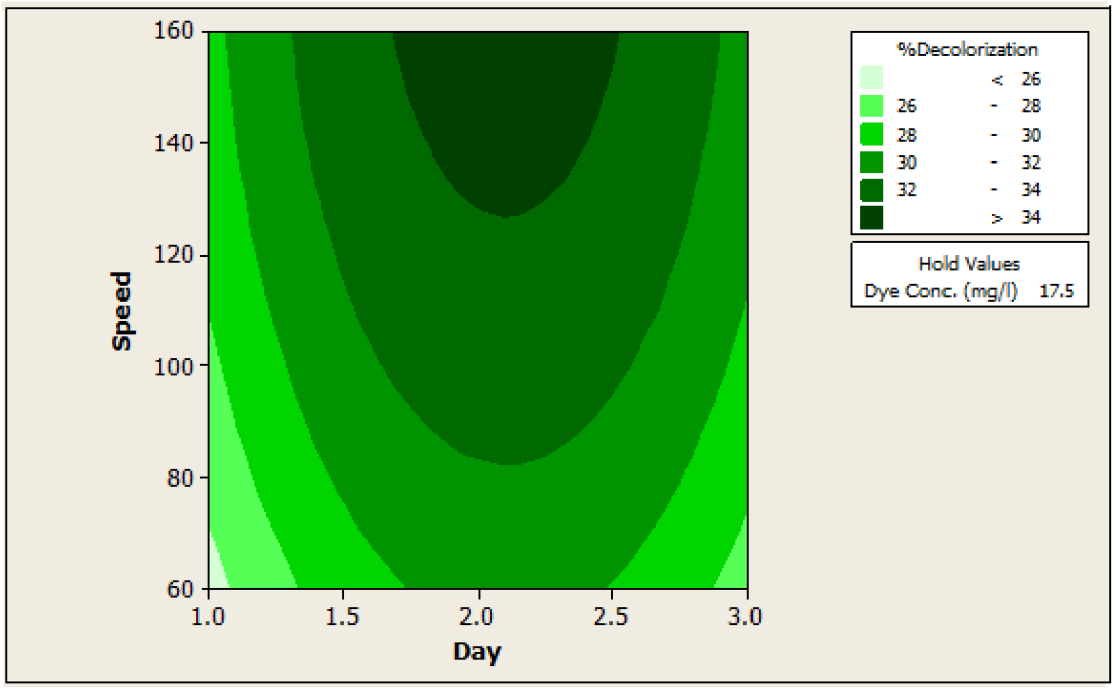

Figure 4.10: Contour plot of agitation speed (rpm) versus process time (day).

From Figure 4.10, the dark green region indicates the highest value of decolorization where feasible optimization can be done. The highest percentage of dye decolorization (> 34%) could be achieved by increasing the agitation speed higher than 130 rpm and process time should be maintained up to 2 days at constant amount of dye concentration (17.5 ppm). However, the variation between speeds did not produced significant effect on percentage of decolorization. Agitation speed of 60 rpm was sufficient (> 30% of percentage of decolorization) to eliminate concentration gradient and promote interchanging between substrate and product from the liquid layer boundary of the beads.

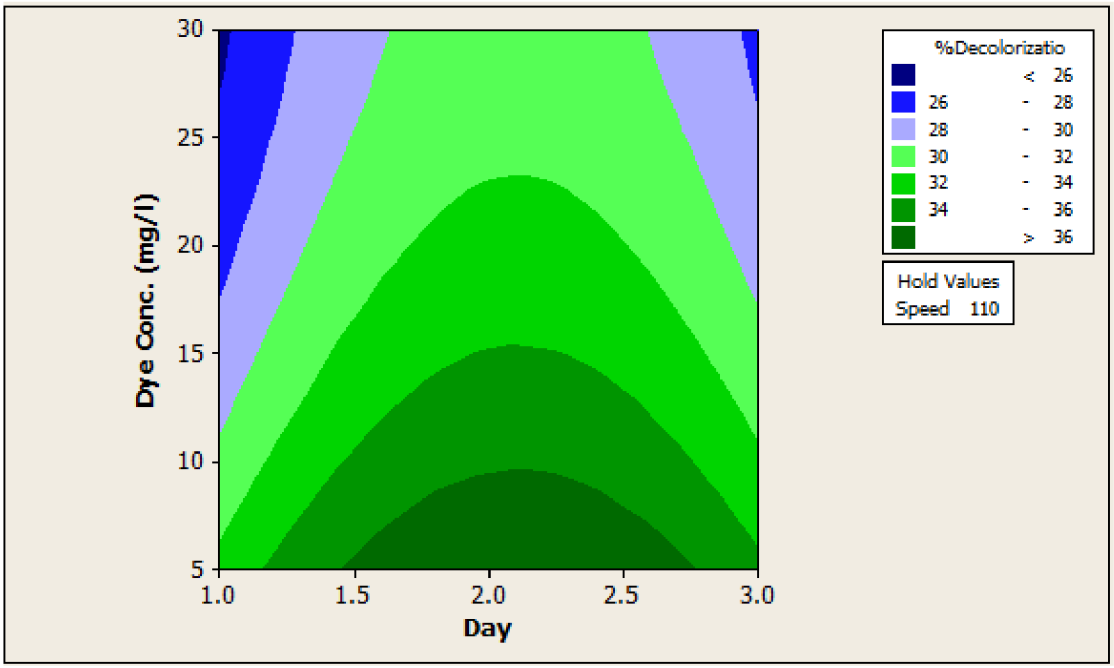

Figure 4.11: Contour plot of initial dye concentration (ppm) versus process time (day).

The effect of initial dye concentration was performed by increasing the crystal violet concentration from 5 to 30 ppm. At constant agitation speed of 110 rpm, the highest percentage of dye decolorization (> 36%) can be achieved at low dye concentration (5 to 10 ppm) and the process time should be maintained up to 2 days. However, less than 30% of colour removal was obtained when the dye concentrations were between 17.5 and 30 ppm. Hence, lower concentration of crystal violet (≤ 10 ppm) and 2 days of process time are advisable to be used to get optimum percentage of decolorization.

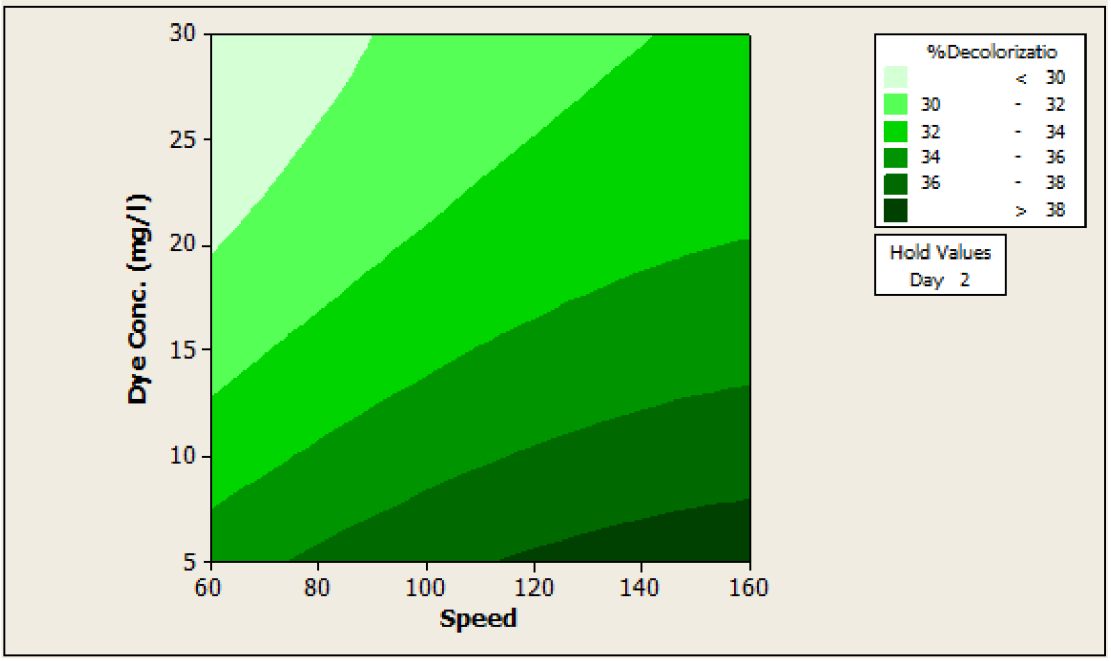

Figure 4.12: Contour plot of initial dye concentration (ppm) versus agitation speed (rpm).

From the contour plot (Figure 4.12), it was observed that at day 2, the highest percentage of decolorization (> 38%) was recorded at dye concentration less than 10 ppm and agitation speed more than 110 ppm. However at 60 rpm, acceptable percentage of dye decolorization (> 34%) can be reached. As 60 rpm is sufficient to get homogenous solution mixture, it is in favor to be used industrially as it can be cost effective and more practical.

4.5.5 RSM optimization prediction

Optimization was carried out by Response Optimization option in the MINITAB®14 software. Details of the optimization were shown as follows:

Optimization goal : To maximize the response (percentage of decolorization)

Lower value : 26%

Upper value : 38%

The optimal values returned by the optimization routine were shown in Table 4.10.

Table 4.10: Optimization values

Local solution			**Predicted responses**		
Speed	**Dye concentration**	**Day**	**% decolorization**	**Desirability**	**Composite desirability**
60.0547	5.0039	1.9381	34.9887	0.99875	0.99875

Global solution			Predicted responses		
Speed	**Dye concentration**	**Day**	**% decolorization**	**Desirability**	**Composite desirability**
60.0547	5.0039	1.9381	34.9887	0.99875	0.99875

Based on Table 4.10, the global solution was found to be the same as local solution indicating that there was only one possible optimal solution. The desirability of the optimum solution was found to be approximately 99%. Thus, the optimization results obtained were: agitation speed 60 rpm, 2 days of process time and initial dye concentration 5 ppm.

Following the optimization, to obtain 35% of crystal violet decolorization, the agitation speed, process time (day) and dye concentration need to be set up at 60 rpm, 2 days and 5 ppm respectively. The composite desirability of this optimization process was 0.99875; it means that for 100 times experimental runs, it is possible to achieve 99 times the targeted dye decolorization.

4.6 Validation of predicted parameters for optimal percentage of decolorization

The subsequent validation experiments were done in triplicate according to the optimal operating values obtained. The validation experiment results obtained were shown in Table 4.11. The average percentage of decolorization obtained was 34.8%. This percentage of decolorization was found to be sufficiently close to the targeted response, thus validating the optimization, *i.e.* the validation results are in close agreement with the model prediction by RSM.

Table 4.11: Dye decolorization under optimized conditions.

Replicate	Percentage of decolorization (%)
1	34.98
2	35.17
3	34.32
Average	**34.82 ± 0.44**
Prediction	**34.99**

4.7 Stirred tank reactor experiments

The stirred tank reactor experiments were done in a total volume of 1 L. The power requirements for both impellers were examined in order to determine which impeller consume less power in pre-determined speed of 60 and 160 rpm and at the same time gives efficient dye decolorization.

4.7.1 Power requirements for mixing

Power requirements for mixing of non-aerated fluids depend on power number, impeller speed, impeller diameter and fluid density. Power consumptions were calculated using Equation (12) and tabulated in Table 4.12.

Table 4.12: Power requirements for different types of impellers at different speeds.

60° axial flat blade impeller		**180° curved blade impeller**	
160 rpm	**60 rpm**	**160 rpm**	**60 rpm**
1.13×10^{-2} W	**6.0×10^{-4} W**	**1.01×10^{-2} W**	**5.0×10^{-4} W**

Based on Table 4.12, 60° axial flat blade impeller seemed to consume similar power as 180° curved blade impeller. For both impellers, higher speed required more power to accelerate the impeller. Therefore, the better type of impeller between the two types used here is solely determined according to the maximum percentage of decolorization, since the power consumption for both types of impellers are almost similar.

4.7.2 Scaling up of dye decolorization experiments

The scaled up experiments were carried out to study the effect of agitation speed, impeller geometry and initial dye concentrations on dye decolorization. Tables 4.13 and 4.14 show the percentage of dye decolorization under different mixing conditions with the two impeller geometries and different speeds.

Table 4.13: Percentage (%) of decolorization for 60° angled flat blade impeller results.

	160 rpm & 30 ppm	**60 rpm & 30 ppm**	**160 rpm & 5 ppm**	**60 rpm & 5 ppm**
Day	**Mean**	**Mean**	**Mean**	**Mean**
0	0	0	0	0
1	16.22	21.70	33.93	28.89
1.5	23.98	23.73	35.36	30.26
2	21.85	24.18	34.97	30.82
2.5	22.03	22.65	35.25	30.97
3	24.09	24.80	35.80	31.57

** Standard deviation of each data point < 0.5%. Each data point was an average of triplicate measurements.*

Table 4.14: Percentage (%) of decolorization for 180° curved blade impeller results.

	160 rpm & 30 ppm	60 rpm & 30 ppm	160 rpm & 5 ppm	60 rpm & 5 ppm
Day	**Mean**	**Mean**	**Mean**	**Mean**
0	0	0	0	0
1	12.73	21.54	24.31	25.82
1.5	12.36	23.97	24.91	26.88
2	15.11	25.02	27.70	26.60
2.5	13.57	24.98	25.94	26.55
3	13.92	25.02	25.78	32.04

** Standard deviation of each data point < 0.5%. Each data point was an average of triplicate measurements.*

4.7.2.1 Effect of impeller geometry

The effect of impeller geometry was observed at speeds of 60 and 160 rpm. In immobilized enzyme systems, the reactants have to diffuse from the bulk liquid to the external surface of the enzyme (Xiong *et al.*, 2008). These transport phenomena can be enhanced at the optimum speed of agitation.

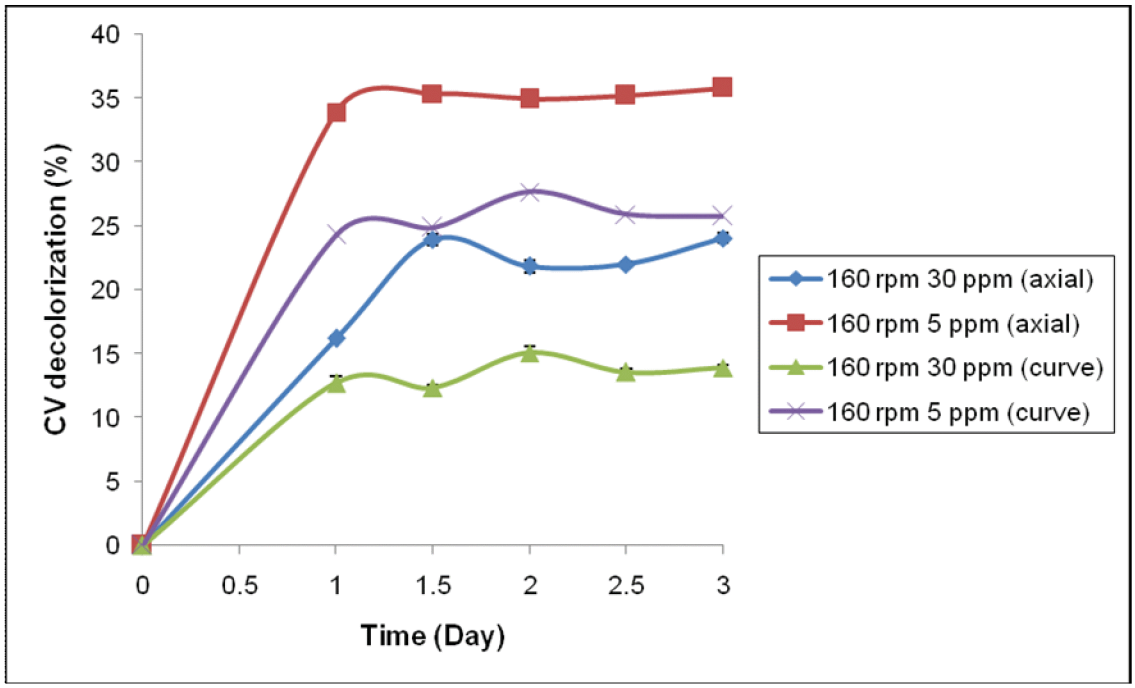

Figure 4.13: Effect of impeller geometry and initial dye concentrations at constant agitation speed of 160 rpm.

Figure 4.13 shows the effect of impeller geometry and initial dye concentrations at constant 160 rpm agitation speed. In this graph, both impeller types show that low dye concentration gives greater percentage of dye decolorization. At the same impeller speed of 160 rpm, the axial impeller (60° angled flat blade) was better than the 180° curved blade impeller (for both low and high dye concentration) in facilitating the dye decolorization process by sodium alginate immobilized laccase.

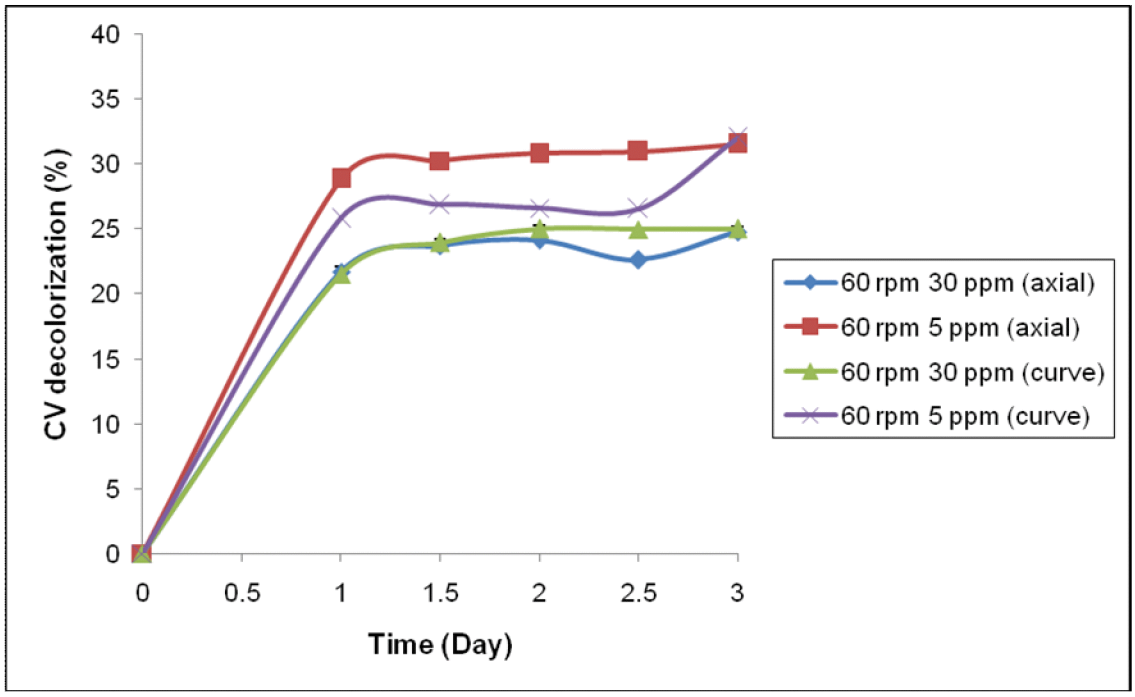

Figure 4.14: Effect of impeller geometry and initial dye concentrations at constant agitation speed of 60 rpm.

At a lower impeller speed of 60 rpm, for both impellers, the lower concentration of dye again gave better percentage of decolorization. Figure 4.14 shows the curves for 5 ppm for both the axial and curved blade being higher than the curves for 30 ppm. The axial impeller also performed better at this speed of 60 rpm for 5 ppm. At 30 ppm initial concentration, there is little different between two impellers with about 24% of decolorization. Comparing Figure 4.13 and 4.14 it can be deduced that at slow impeller speed and high concentration of dye, the axial and curved blade did not show significant difference on dye decolorization but at low dye concentration of 5 ppm at 60 rpm, the axial impeller produced better decolorization compared to the curved blade. At the higher

speed of 160 rpm the axial impeller showed significantly better decolorization for both initial concentrations.

4.7.2.2 Effect of agitation speeds

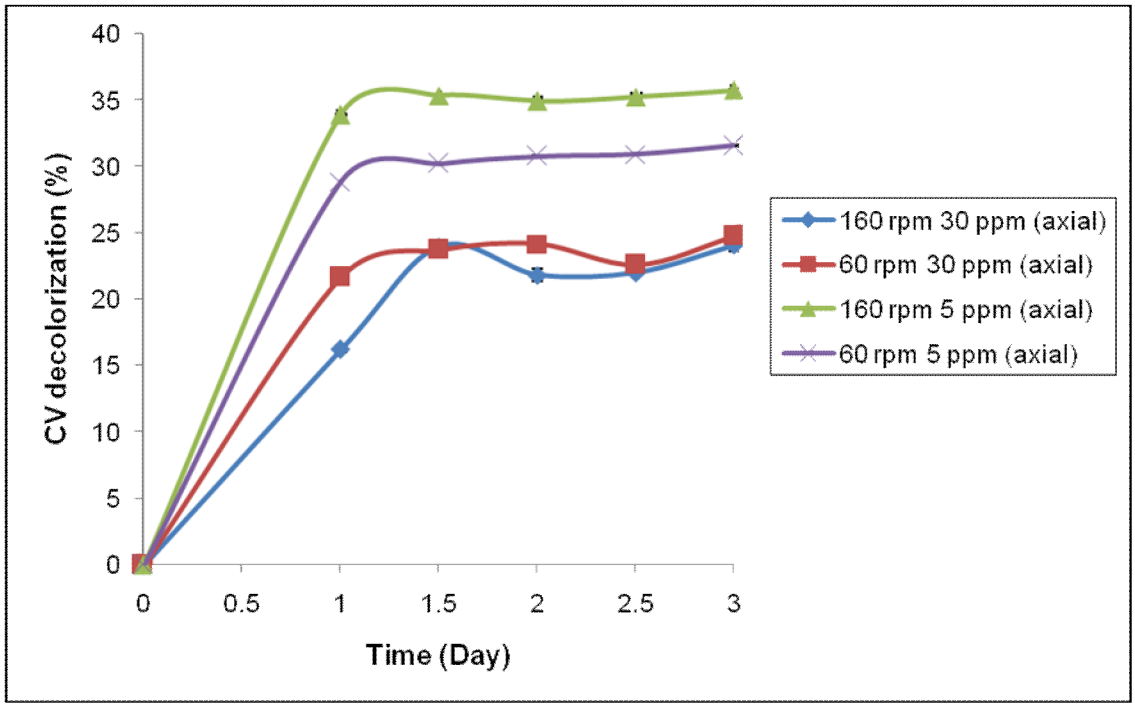

Figure 4.15: Effect of agitation speeds and initial dye concentrations for 60° axial flat blade impeller in crystal violet decolorization.

In Figure 4.15 for axial impeller, at the low dye concentration 5 ppm, the impeller speed of 160 rpm result in 36% of dye decolorization while at the lower speed (60 rpm) the decolorization was 31%. For the higher dye concentration of 30 ppm, the speed of the impeller did not seem to have significant effect on the percentage of decolorization as both speeds (60 & 160 rpm) resulted in approximately 24% of dye decolorization. These data shows for the axial impeller, impeller speed may be important at a low dye

concentration, but the significance appears to be diminished at higher initial concentration.

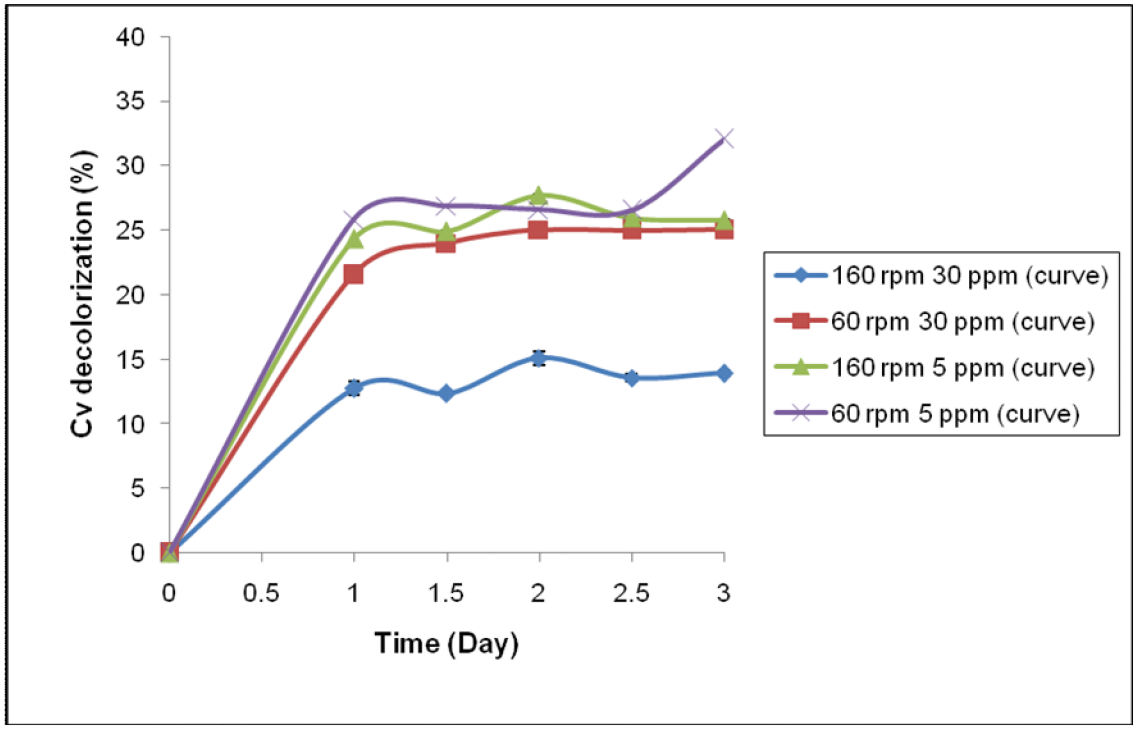

Figure 4.16: Effect of agitation speeds and initial dye concentrations for 180° curved blade impeller in crystal violet decolorization.

In contrast, for 180° curved blade impeller (Figure 4.16), at the low dye concentration of 5 ppm, the impeller speed did not have significant effects towards dye decolorization. The percentage of dye decolorization for 60 and 160 rpm for 5 ppm were approximately the same which was around 27% of decolorization. However, at 30 ppm dye concentration, the speed of impeller was important with the lower speed of 60 rpm result in greater dye decolorization (24%) compared the higher speed (13%). Hence, for curved blade, if low concentration of dye is used, the speed of the impeller is not crucial

because the outcome would be quite similar, conversely, if higher concentration of dye is used, the speed of the impeller must be low to give optimum percentage of decolorization.

4.7.2.3 Effect of initial dye concentration concentrations

The effect of crystal violet concentration was studied over the range of 5–30 ppm by keeping the enzyme quantity constant. Figure 4.17 compares each decolorization progress curve at constant substrate concentration.

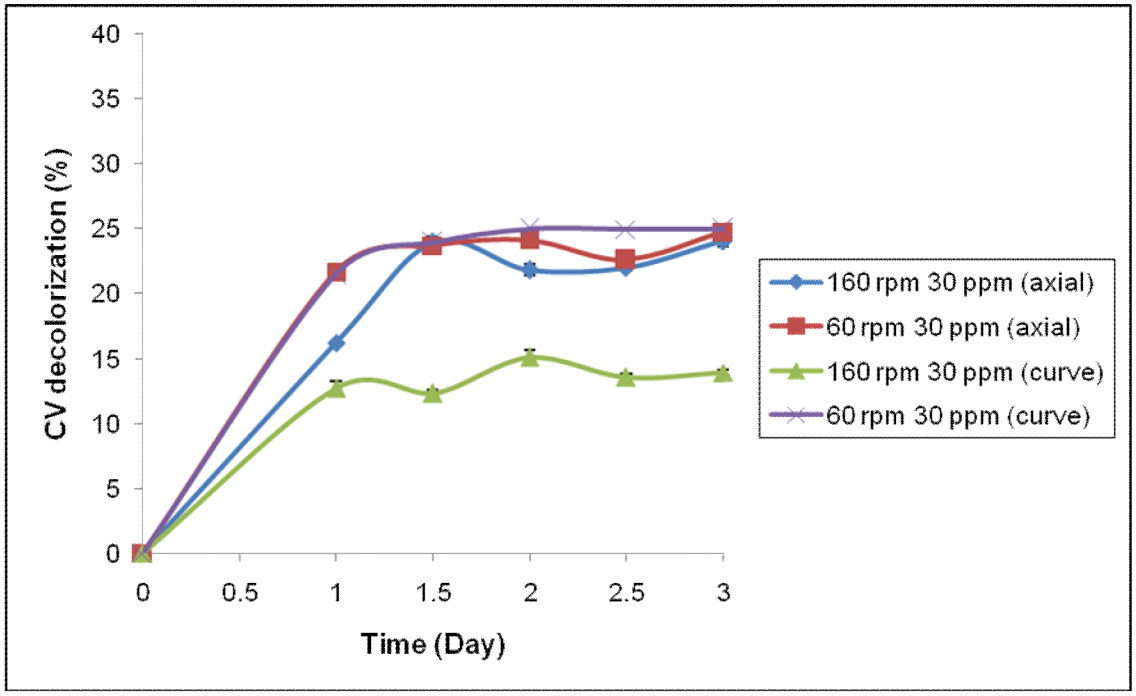

Figure 4.17: Effect of initial dye concentration (30 ppm) for crystal violet decolorization.

For the axial impeller, the speed of the impeller did not give significant effect at high concentration of dye (30 ppm) where both result in 24% of dye decolorization. However, for curved-blade impeller, at high concentration of dye, the lowest speed of impeller (60 rpm) seemed to facilitate dye decolorization (24%) as compared to higher 160 rpm which result in low percentage of dye decolorization (13%).

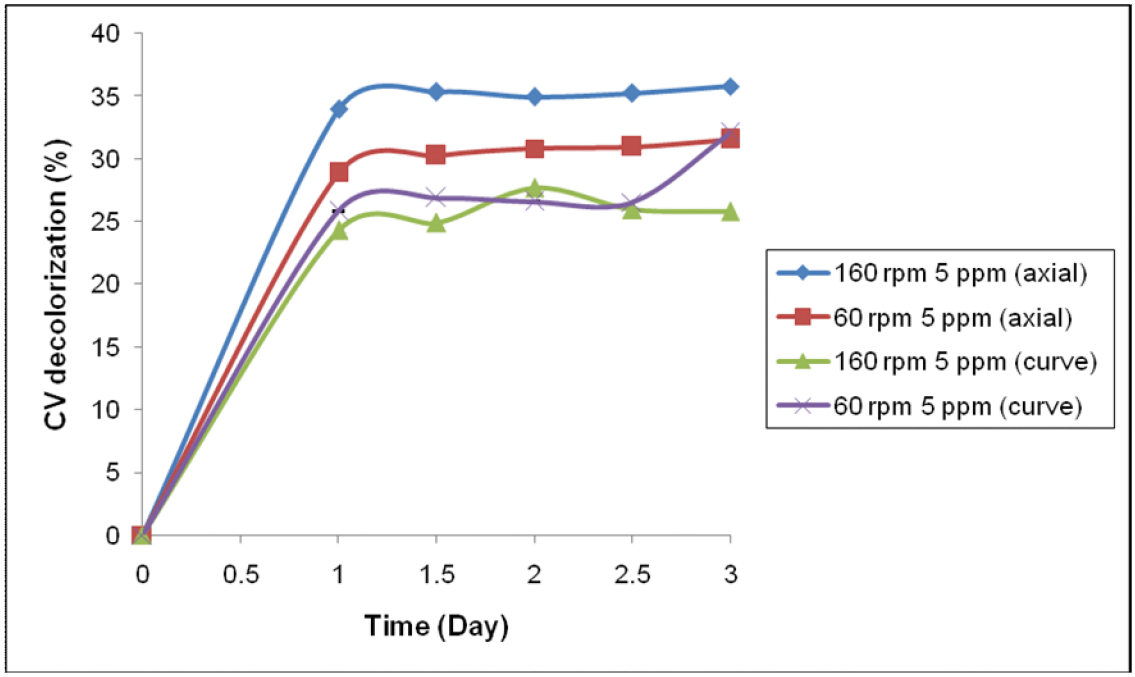

Figure 4.18: Effect of initial dye concentration (5 ppm) for crystal violet decolorization.

At low dye concentration, high axial impeller speed gave greater impact towards dye decolorization (36%) as compared to lower speed (31%). On the other hand, the for curve impeller, low dye concentration did not give significant effect towards dye decolorization even if impeller speed was higher, the percentage of decolorization were almost the same for both speed (27%).

The results for this work have shown that mixing can have effects on dye decolorization process in a stirred tank. The impeller geometry, speed and initial dye concentration are parameters that have shown impact on the process. Both the impellers used, a 60° angled blade pumping down and a curved blade pumping radially were estimated to have similar power requirement at the speed studied. Hence, their performance was measured based on the percentage of decolorization achieved at the same speed and time of mixing. Under different condition of speed and initial concentrations, the axial impeller was able to give better decolorization percentage than the curved blade.

Summary of STR experiments observations are as follows:

Table 4.15: General comparisons of stirred tank reactor experiments.

Impeller geometry \ Parameter	Percentage of crystal violet decolorization (%)		
	Speed (rpm)	Initial dye concentration (ppm)	
		5	30
60° axial flat blade impeller	60	2.531%	2.6 24%
	160	2.736%	2.8 24%
180° curved blade impeller	60	2.927%	2.10 24%
	160	2.11 27%	2.12 13%

1) 60° axial flat blade impeller

   I. At low initial concentration of dye (5 ppm), the agitation speed must be high (160 rpm) to get maximum percentage of decolorization;

   II. At high initial concentration of dye (30 ppm), the agitation speed did not have significant effect towards dye decolorization, hence, lower speed is encouraged to be used for high initial dye concentration as it can save operational cost;

   III. At high speed (160 rpm), axial impeller is better compared to curved blade for both high (30 ppm) and low (5 ppm) initial dye concentration;

   IV. At low speed (60 rpm), axial is better than curved blade for low initial dye concentration (5 ppm), however, at high initial dye concentration (30 ppm) there was no significant effect in dye decolorization for both impellers.

2) 180° curved blade impeller

   I. At low initial dye concentration (5 ppm), the agitation speed did not pose significant effect towards dye decolorization;

   II. At high initial dye concentration (30 ppm), the lower agitation speed (60 rpm) gave higher percentage of decolorization compared to higher speed of agitation (160 rpm).

In all cases, low initial dye concentration was observed to give greater percentage of decolorization compared to higher initial dye concentration.

CHAPTER 5

CONCLUSIONS AND FUTURE CONSIDERATIONS

5.1 Conclusions

- Assay time for free laccase was determined at 10 minutes.

- The V_{max} and K_m values obtained were approximately 9.82 ± 0.03 μM min^{-1} and 0.0188 ± 0.001 mM respectively.

- The optimum conditions for laccase immobilization were found to be at 2% w/v alginate solution, 2% w/v calcium chloride solution and 1:1 ratio of enzyme to alginate solution with immobilization efficiency was found to be around 90% and small lag time approximately 20 minutes. Consistent beads with diameter of 2.5 ± 0.5 mm were produced.

- The optimal conditions for crystal violet decolorization were found to be at 5 ppm, 2 days and 60 rpm. These values are based on optimal setting points of process parameters derived from RSM optimization design (Box-Behnken) using 2 Units enzyme amount and at room temperature (25 ± 1°C). The speed was defined as statistically insignificant for the experiment. Hence, the agitation speed was set at lowest speed (60 rpm) in subsequent validation experiments. The predicted results were in closed agreement with the results obtained from actual experimental results *i.e.* 34.822 ± 0.444 %.

- With approximately same power consumption for both impellers (60° angled axial and 180° curved blade), axial impeller performed better than curved blade impeller. By choosing the right impellers, the percentage of crystal violet decolorization can be maximized and save the power consumption.

5.2 Future considerations

The results demonstrated that immobilized laccase from *Trametes versicolor* has potential application in dyestuff treatment and constitute a promising alternative for wastewater remediation and making it an economically viable choice. The findings from this experiment open up further opportunities for other types of dye or mixture of dyes to be treated with laccase from *Trametes versicolor*.

REFERENCES

Abadulla, E., Tzanov, T., Costa, S., Robra, K. H., Paulo, A. C. and Gubitz, G. M. (2000). Decolorization and detoxification of textile dyes with a laccase from *Trametes hirsute*. *Appl. Environ. Microbiol.* 66(8): 3357–3362.

Antorini, M., Gimbert, I. H., Choinowski, T., Sigoillot, J. C., Asther, M., Winterhalter, K. and Piontek, K. (2002). Purification, crystallisation and X-ray diffraction study of fully functional laccases from two ligninolytic fungi. *Biochimica et Biophysica Acta*. 1594: 109–114.

Aslan, N. and Cebeci, Y. (2007). Application of Box–Behnken design and response surface methodology for modeling of some Turkish coals. *Fuel*. 86: 90–97.

Aziz, A. A. R. (2007). Hydrodynamics and mass transfer characteristics of curved blade impellers for multiphase mixing in stirred vessels. Ph. D Thesis: University Malaya.

Bhattacharya, S.S. and Banerjee, R. (2008). Laccase mediated biodegradation of 2,4-dichlorophenol using response surface methodology. *Chemosphere*. 73: 81–85.

Cameselle, C., Pazos, M., Lorenzo, M. and Sanroman, M. A. (2003). Enhanced decolourisation ability of laccase towards various synthetic dyes by an electrocatalysis technology. *Biotechnol. Letters*. 25: 603–606.

Cho, N. S., Wilkolazka, A. J., Luterek, J., Cho, H. Y., Ohga, S. and Leonowicz, A. (2006). Effect of fungal laccase and low molecular weight mediators on decolorization of Direct Blue dye. *J. Fac. Agr., Kyushu Univ.* 51 (2): 219–225.

Claeyssens, M., Tilbeurgh, H., Tomme, P., Wood, M. T. & McRae, I. S. (1989) Fungal cellulase systems: comparison of the specificities of the cellobiohydrolases isolated from *Penicillium pinophilum* and *Trichoderma reesei. Biochem. J.* 261: 819-825.

Couto, S. R. and Toca Herrera, J. L. (2006). Industrial and biotechnological applications of laccases: A review. *Biotechnol. Adv.* 24: 500–513.

Couto, S. R. (2007). Decolouration of industrial azo dyes by crude laccase from *Trametes hirsute*. *J. Hazard. Mater.* 148: 768–770.

D'Souza, D. T., Tiwari, R., Sah, A. K. and Raghukumara, C. (2006). Enhanced production of laccase by a marine fungus during treatment of colored effluents and synthetic dyes. *Enzyme Microb.Technol.* 38: 504–511.

Doran, P.M. (1995). *Bioprocess Engineering Principles*. London: Academic Press Limited.

Glanville, S. D. and Clark, A. G. (1997). Inhibition of human glutathione-s-transferases by basic triphenylmethane dyes. *Life Sci.* 60(18): 1535-1544.

Haaland, P.D. (1989). *Experimental design in biotechnology*. New York: Marcel Dekker.

Ibrahim, S. and Nienow, A. W. (1995). Power curves and flow patterns for a range of impellers in Newtonian fluids: $40 < Re < 5 \times 10^5$. *Trans IChemE.* 73: 485-491.

Ivan, V. A. and Robert, M. J. C. (1994). *Immobilized Biosystems*. Theory and practical application. 32–45.

Kandelbauer, A., Maute, O., Kessler, R. W., Erlacher, A. and Gubitz, G. M. (2004). Study of dye decolorization in an immobilized laccase enzyme-reactor using online spectroscopy. *Wiley InterScience* (www.interscience.wiley.com). DOI: 10.1002/bit.20162 (552–563).

Kunamneni, A., Ghazi, I., Camarero, S., Ballesteros, A., Plou, F. J. and Alcalde, M. (2008). Decolorization of synthetic dyes by laccase immobilized on epoxy-activated carriers. *Process Biochem.* 43: 169–178.

Lu, L., Zhao, M. and Wang, Y. (2007). Immobilization of laccase by alginate–chitosan microcapsules and its use in dye decolorization. *World J. Microbiol. Biotechnol.* 23: 159–166.

Maddhinni, V.L., Vurimindi H. B. and Yerramilli, A. (2006). Degradation of azo dye with Horse Radish Peroxidase (HRP). *J. Indian Inst. Sci.* 86: 507–51.

Mayer, A. M. and Staples, R. C. (2002). Laccase: a new function for an old enzyme. *Phytochemistry*. 60: 551–565.

Mechichi, T., Mhiri, N. and Sayadi, S. (2006). Remazol Brilliant Blue R decolourization by the laccase from *Trametes trogii*. *Chemosphere*. 64: 998–1005.

Montgomery, D. C. (2001). *Design and Analysis of Experiment (5th Edition)*. USA: John Wiley & Sons, Inc.

Mosbach, K. (1987). *Methods in enzymology*. Vol. 135, New York: Academic Press Limited.

Muthukumar, M., Sargunamani, D. and Selvakumar, N. (2005). Statistical analysis of the effect of aromatic, azo and sulphonic acid groups on decolouration of acid dye effluents using advanced oxidation processes. *Dyes and Pigments*. 65: 151-158.

Niladevi, K. N. and Prema, P. (2008). Effect of inducers and process parameters on laccase production by *Streptomyces psammoticus* and its application in dye decolourization. *Bioresource Technol*. 99: 4583–4589.

Nilsson, K. (1987). Methods for immobilizing animal cells. *Trends in Biotechnol*. 5: 73–78.

Nogala, W., Rozniecka, E., Rogalski, J. and Opallo, M. (2007). pH-Sensitive syringaldazine modified carbon ceramic electrode for bioelectrocatalytic dioxygen reduction. *J. Electroanalytical Chem.* 608: 31–36.

Norton, S., Lacroix, C., Vuillemard, J. (1994) Kinetic study of continuous whey permeate fermentation by immobilized *Lactobacillus helveticus* for lactic acid production. *Enzyme Microb. Technol.* 16: 457–466.

Park, H. J. and Khang, Y. H. (1995). Production of cephalosporin C by immobilized *Cephalosporin acremonium* in polyethyleneimine-modified barium alginate. *Enzyme Microb. Technol.* 17: 408–412.

Pointing, S. B. and Vrijmoed, L. L. P. (2000). Decolorization of azo and triphenylmethane dyes by *Pycnoporus sanguineus* producing laccase as the sole phenoloxidase. *World J. Microbiol. & Biotechnol.* 16: 317–318.

Sattler, W., Esterbauer, H., Glatter, O. & Steiner, W. (1989) The effect of enzyme concentration on the rate of the hydrolysis of cellulose. *Biotechnol. Bioeng.* 33:1221-1234.

Schliephakea, K., Mainwaringb, D. E., Lonergana, G. T., Jonesa, I. K. and Baker, W. L. (2000). Transformation and degradation of the disazo dye Chicago Sky Blue by a purified laccase from *Pycnoporus cinnabarinus. Enzyme Microb. Technol.* 27: 100–107.

Schmid, F. X. (2001). Biological macromolecules: UV-visible spectrophotometry. *Encyclopedia of life sci*. Macmillan Publishers Ltd.

Segel, I. H. (1975). *Enzyme kinetics: Behavior and analysis of rapid equilibrium and steady state enzyme systems*. USA: John Wiley and Sons.

Shacham, M. and Brauner, N. (2008). Preventing oscillatory behavior in error control for ODEs. *Comp. Chem. Engin*. 32: 409-419.

Sriamornsak, P. and Sungthongjeen, S. (2007). Modification of Theophylline release with alginate gel formed in hard capsules. *AAPS PharmSciTech*. 8 (3) Article 51: E1-E8.

Srikanlayanukul, M., Khanongnuch, C. and Lumyong, S. (2006). Decolorization of textile wastewater by immobilized *Coriolus versicolor* RC3 in repeated-batch system with the effect of sugar addition. *J. Chiang Mai Uni.* 5(3): 301–306.

Stolz, A. (2001). Basic and applied aspects in the microbial degradation of azo dyes. *Appl. Microbiol. Biotechnol.* 56: 69–80.

Tauber, M. M., Guebitz, G. M. and Rehorek, A. (2005). Degradation of azo dyes by laccase and ultrasound treatment. *Appl. Environ. Microbiol.* 71 (5): 2600–2607.

Tavares, A. P. M., Cristóvão, R. O., Loureiro, J. M., Boaventura, R. A. R, and Macedo E. A. (2009). Application of statistical experimental methodology to optimize reactive dye decolourization by commercial laccase. *J. Hazard. Mater.* 162: 1255–1260.

Trovaslet, M., Enaud, E., Guiavarch, Y., Corbisier, A. M and Vanhulle, S. (2007). Potential of a *Pycnoporus sanguineus* laccase in bioremediation of wastewater and kinetic activation in the presence of an anthraquinonic acid dye. *Enzyme Microb. Technol.* 41: 368–376.

Vanhulle, S., Enaud, E., Trovaslet, M., Nouaimeha, N., Bols, C. M., Keshavarz, T., Tron, T., Sannia, G. and Corbisier, A. M. (2007). Overlap of laccases/cellobiose dehydrogenase activities during the decolourisation of anthraquinonic dyes with close chemical structures by *Pycnoporus* strains. *Enzyme Microb. Technol.* 40: 1723–1731.

Wesenberg, D., Kyriakides, I. and Agathos, S. N. (2003). White-rot fungi and their enzymes for the treatment of industrial dye effluents. *Biotechnology Advances.* 22: 161-187.

Won, K., Kim, S., Kim, K.J., Park, H.W. and Moon, S.J. (2005). Optimization of lipase entrapment in Ca–alginate gel beads. *Process Biochem.* 40: 2149–2154.

Xiong, J., Wu, J., Xu, G. and Yang, L. (2008). Kinetic study of lipase catalyzed asymmetric transesterification of mandelonitrile in solvent-free system. *Chem. Engin. J.* 138: 258–263.

Yesilada, O. and Ozcan, B. (1998). Decolorization of Orange II dye with the crude culture filtrate of white rot fungus, *Coriolus versicolour*. *Turkey J. Biology*. 22: 463–476.

Zille, A., Tzanov, T., Gubitz, G. M. and Paulo, A. C. (2003). Immobilized laccase for decolourization of Reactive Black 5 dyeing effluent. *Biotechnol. Letters*. 25: 1473–1477.